DMD Fast Forward. Published on October 1, 2009 as doi:10.1124/dmd.109.028290
This article has not been copyedited and formatted. The final version may differ from this version.

Inhibition of CYP3A by Erythromycin:

In Vitro-In Vivo Correlation in Rats

Xin Zhang[1], Raymond E. Galinsky, Robert E. Kimura, Sara K. Quinney[2], David R. Jones and Stephen D. Hall[1]

Departments of Pharmacy Practice (X.Z.) and Industrial & Physical Pharmacy (R.E.G.),School of Pharmacy and Pharmaceutical Sciences, Purdue University, West Lafayette, Indiana,

Section of Neonatology, Department of Pediatrics, Rush University Medical Center, Chicago, Illinois (R.E.K.) and Division of Clinical Pharmacology, Department of Medicine, Indiana University School of Medicine, Indianapolis, Indiana (X.Z., R.E.G., S.K.Q., D.R.J., S.D.H)

DMD Fast Forward. Published on October 1, 2009 as DOI: 10.1124/dmd.109.028290
This article has not been copyedited and formatted. The final version may differ from this version.

Running Title: *In vitro-in vivo* correlation of CYP3A inhibition

Address Correspondence to: Xin Zhang, Ph.D

Eli lilly and Company

Lilly Corporate Center

Drop Code 0734

Indianapolis, IN 46285

Phone: 317-276-3757

Fax: 317-433-6661

E-mail: zhangxx@lilly.com

Text page: 40

Tables: 4

Figures: 7

Abstract: 234 words

Introduction: 644 words

Discussion: 1581 words

Abbreviations

MIC: metabolic intermediate complex; MBI: mechanism-based inhibition; ERY: erythromycin; MDZ: midazolam; DDI: drug-drug interaction; RLM: rat liver microsome; PBPK: physiologically-based pharmacokinetic modeling.

DMD Fast Forward. Published on October 1, 2009 as DOI: 10.1124/dmd.109.028290
This article has not been copyedited and formatted. The final version may differ from this version.

Abstract

The prediction of *in vivo* drug-drug interactions from *in vitro* enzyme inhibition parameters remains challenging, particularly when time-dependent inhibition occurs. This study was designed to examine the accuracy of *in vitro*-derived parameters for the prediction of inhibition of CYP3A by erythromycin (ERY). Chronically-cannulated rats were employed to estimate the reduction in *in vivo* and *in vitro* intrinsic clearance (CL_{int}) of midazolam (MDZ) following single and multiple doses of ERY; *in vitro* recovery of CL_{int} was determined at 1, 2, 3 and 4 days after discontinuation of ERY. Enzyme inhibition parameters (k_{inact}, K_I, and K_i) of ERY were estimated *in vitro* using untreated rat liver microsomes. *In vivo* enzyme kinetic analysis indicated that single and multiple doses of ERY (100 mg/kg i.v. infusion over 4 hrs) reduced MDZ CL_{int} by reversible and irreversible mechanisms, respectively. CYP3A inactivation after multiple doses of ERY treatment reflected metabolic intermediate complex (MIC) formation without a significant change in hepatic CYP3A2 mRNA. A physiologically-based pharmacokinetic (PBPK) model of the interaction between ERY and MDZ predicted a 2.6-fold decrease in CYP3A activity following repeated ERY treatment using *in vitro*-estimated enzyme inhibition parameters and *in vivo* degradation half-life of the enzyme (20 ± 6 hr). The observed fold decreases were 2.3-fold and 2.1-fold for the *in vitro*-estimated CYP3A activity and the *in vivo* CL_{int} , respectively. This study demonstrates that *in vivo* DDIs are predictable from *in vitro* data when the appropriate model and parameter estimates are available.

DMD Fast Forward. Published on October 1, 2009 as DOI: 10.1124/dmd.109.028290
This article has not been copyedited and formatted. The final version may differ from this version.

Introduction

The prediction of *in vivo* drug-drug interactions (DDIs) from *in vitro* data has met with limited success and the general applicability of such predictions is unclear (Obach et al, 2005; Wang et al., 2004; Obach et al., 2007; von Moltke et al., 1998). As drugs capable of mechanism-based inhibition (MBI) have emerged as clinically important cytochrome P450 CYP3A (CYP3A) inhibitors (Zhou, et al., 2006) the uncertainty in predictive accuracy has increased. Approaches to predicting MBI based DDIs vary from a relatively simple method using a single inhibitor concentration to more complicated physiologically-based pharmacokinetic (PBPK) models that consider the change of inhibitor and substrate concentrations with time (Mayhew et al., 2000; Wang et al., 2004; Obach et al., 2007; Ito et al., 2003). Changes in the amount of active enzyme in the presence of a mechanism-based inhibitor are estimated using the *in vitro* enzyme inactivation parameters, K_I and $k_{inact,}$ which can be used to predict the increase in the *in vivo* exposure of the substrate. These predictions often suffer from poor characterization of substrate and inhibitor properties *in vitro* and/or *in vivo* and from uncertainties in predictive model parameter values. For example, DDIs may reflect simultaneous reversible inhibition, irreversible inhibition and induction at multiple sites of enzyme expression but the relative contribution of each type of interaction *in vivo* may be difficult to define. PBPK models provide a manageable path forward for addressing these potentially complex DDIs and have the important advantage of accommodating the mutual, nonlinear interactions between inhibitors and substrates. However, these approaches are based on the often untested assumption that mechanisms and potencies of interactions can be readily translated form *in vitro* systems to the whole animal.

The most common locus of DDIs is the CYP family of enzymes and the CYP3A sub-family in particular. Midazolam (MDZ) is the most common substrate used to characterize CYP3A activity in humans and rats because of its high CYP3A selectivity and its lack of significant interaction with cell membrane transporters (Franke et al., 2008). CYP3A2 and CYP2C11 are the major P450 isoforms found in male rat liver (Shaw et al., 2002) and MDZ is almost exclusively metabolized by CYP3A2 to form primarily 4-OH MDZ (Shaw et al 2002 and Uhing et al., 2004).

The effect of erythromicin (ERY) administration on CYP3A activity is complex and potentially reflects the net effect of enzyme induction, reversible inhibition and irreversible inhibition (Amacher et al., 1991; Danan et al., 1981; Yamano et al., 2000). ERY, a tertiary amine, forms a stable metabolic intermediate complex (MIC) *in vivo*, that displays a characteristic Soret peak around 456 nm, and inactivates CYP3A (Pershing et al., 1982). Approximately 40% of total CYP forms MIC following daily oral administration of 800 mg of ERY to humans (Amacher et al., 1991). Interestingly, no complex could be detected in human liver microsomes isolated following a single oral dose of ERY (Danan et al., 1981; Yamano et al., 2000). It has been suggested that chronic ERY administration is capable of inducing CYPs. For example, repeated oral administration of ERY, 2 mmol/kg daily for four days in humans increased hepatic microsomal protein concentration as well as ERY N-demethylase activity (Danan et al., 1981). In contrast, several other studies have reported no induction following chronic ERY treatment in rats (Yamano et al., 2000; Takedomi et al., 2001).

In this study we examined the interaction between MDZ and ERY using a previously validated, physiologically stable chronically cannulated rat model that allows these complex interactions to be quantified *in vivo*. (Uhing et al., 2004, Quinney et al, 2008) The *in vitro* parameters characterizing reversible and irreversible components of

CYP3A inhibition by ERY were determined using hepatic microsomes from rats treated with ERY. Finally we developed a physiological model for quantitatively predicting the magnitude of the *in vivo* changes in intrinsic clearance of MDZ based upon in vitro estimated enzyme inhibition parameters.

Materials and Methods

Chemicals

MDZ (Versed™; Roche Pharma Inc., Switzerland) was diluted in sterile saline to the desired concentrations before i.v. administration. Sterile erythromycin lactobionate (Erythrocin, Abbott Laboratories, Abbott Park, IL) was reconstituted in 5 percent dextrose injection (Uhing et al., 2004).

Animals

Male Sprague-Dawley rats weighing 325 to 350 g were obtained from Charles River Laboratories, Inc. (Wilmington, MA). Rats were housed individually in standard cages and were allowed free access to water and food pellets. Animals were maintained under constant temperature and humidity and a daily 14/10-hr light/dark cycle. The drug disposition studies were performed in free-moving, anaesthetized animals. They remained calm in their cages where their behavior was placid during the experimental procedures of drug administration and blood withdrawal. The experimental protocol was approved by the Institutional Animal Care and Use Committee of Rush Medical Center.

Placement of the Catheters

Rats were anesthetized with a mixture of ketamine (60 mg/kg) and xylazine (5 mg/kg) administered intramuscularly. Catheters were placed in the aorta, inferior vena cava and hepatic vein as previously described (Uhing et al., 2004).

In Vivo Pharmacokinetics

The disposition of MDZ following intravenous administration was used as a surrogate for *in vivo* hepatic CYP3A activity (Uhing et al., 2004). Animals were divided into four groups, as described below, and received single or multiple treatments of ERY designed to reversibly or irreversibly inhibit CYP3A activity. The pharmacokinetics of

MDZ were characterized in all animals following intravenous administration of MDZ. All experiments began four days after catheter implantation to allow animals to completely recover from the effect of surgery and anesthesia.

Irreversible CYP3A inhibition was studied in the first group of animals (n=9) following multiple doses of ERY. MDZ (5 mg dissolved in 1 mL of normal saline) was administered via the inferior vena cava by a constant infusion over two minutes. Simultaneous blood samples were obtained from the aorta and hepatic vein (0.2 mL) at 5, 7.5, 10, 15, 20, 30, 45, 60, 90, 120 and 180 minutes after the start of infusion for the determination of baseline MDZ clearance. One day later and daily for four successive days, 150 mg of ERY was administered by infusion over six hours via the inferior vena cava. Hepatic vein blood samples were obtained at 0, 3.5, 4.5, and 5.5 hours after the start of the infusion on each day and assayed for plasma ERY concentrations. At the midpoint of the final ERY infusion, *i.e.* at 3 hours, on day 4, MDZ disposition was determined as previously described. Then, on days one, two, and three following the last dose of ERY, animals (n=3) were sacrificed and their livers obtained to quantify CYP3A activity *in vitro*. A second group of animals (n=3) were sacrificed on the fourth day of ERY treatment, 3 hours after the start of the final ERY infusion in order to obtain control livers not exposed to MDZ.

Competitive inhibition was examined in a third group of rats (n=3). A single dose of ERY (150 mg infused over six hours) was administered intravenously via the inferior vena cava. MDZ (5 mg dissolved in 1 mL of normal saline) was administered at the midpoint of ERY infusion via the inferior vena cava by a constant infusion over two minutes. MDZ disposition was determined as previously described. Livers were obtained immediately upon discontinuation of ERY.

DMD Fast Forward. Published on October 1, 2009 as DOI: 10.1124/dmd.109.028290
This article has not been copyedited and formatted. The final version may differ from this version.

The final group of rats (n = 3) underwent sham surgery and served as controls. Rats received saline infusions identical to ERY administration, i.e. a 1 mL infusion via the inferior vena cava over two minutes for four days, Livers were removed at the end of saline infusion on Day 4.

In all studies, after each blood sample withdrawal, animals were immediately transfused with an equal volume of blood obtained from another set of healthy, chronically catheterized male Sprague-Dawley rats. The hematocrit in all study animals remained stable over the time course of drug administration and blood sample withdrawal.

Sample Size Justification

A previous study indicated that the coefficient of variation of MDZ intrinsic clearance (CL_{int}) was approximately 7.7% (Yamano et al., 2000). With this coefficient of variation and three rats in each group, there is 80% power to detect a difference of 25 mL/min/kg in the CL_{int} of MDZ, at a significance level of 0.05.

The MDZ PK Model

A compartmental pharmacokinetic model was developed to describe MDZ disposition, as illustrated in Fig. 1. The differential equations describing MDZ concentrations in each compartment are shown below and account for mass balance.

$$\frac{dC_A}{dt} = \frac{R_0}{V_C} + \frac{Q_H \times (C_{HV} - C_A)}{V_C} - k_{12} \times C_A + k_{21} \times C_{PER} \times \frac{V_{PER}}{V_C} \quad \text{Eq. 1}$$

$$\frac{dC_{HV}}{dt} = \frac{Q_H \times (C_A - C_{HV})}{V_H} - \frac{V_{max} \times C_{HV}}{K_m + C_{HV}} \quad \text{Eq. 2}$$

$$\frac{dC_{PER}}{dt} = k_{12} \times C_A \times \frac{V_C}{V_{PER}} - k_{21} \times C_{PER} \quad \text{Eq. 3}$$

where, C_A, C_{HV}, and C_{PER} are concentrations in the central compartment (i.e. aorta), the liver (i.e. hepatic vein), and the peripheral compartment, respectively. This approach is based on the well-stirred model (Rowland et al., 1973) and assumes that drug concentration in the liver is in instantaneous equilibrium with drug concentration in the hepatic vein. R_0 is the infusion rate of MDZ. V_C, V_{PER} and V_H are the volume of central compartment, peripheral compartment, and liver, respectively. Q_H is liver blood flow. k_{12} and k_{21} are the distribution rate constants for drug transfer between central and peripheral compartments. V_{max} and K_m are the maximal rate of metabolism and the Michaelis-Menten constant for MDZ.

To test whether the base model (Eq. 1-3) could be reduced to better fit the data, the macro-constants A, B, α, and β for a classical , two-compartment iv infusion pharmacokinetic model were obtained by curve-stripping of the individual MDZ blood concentration time data. V_C and V_{PER} were calculated using equations listed in the Appendix (Eq. A1-A6). This compartmental analysis revealed that the values (mean ± SD) of volume of central and peripheral compartment were not significantly different based on paired Student's t-test: V_C = 526 ± 133 mL, V_{PER} = 478 ± 166 mL (n = 14, p = 0.44). Therefore Eq. 1 and 3 in the MDZ PK model were simplified to Eq. 1' and 3', which improved the precision in the estimation of the model parameters.

$$\frac{dC_A}{dt} = \frac{R_0}{V_C} + \frac{Q_H \times (C_{HV} - C_A)}{V_C} - k_{12} \times C_A + k_{21} \times C_{PER} \qquad \text{Eq. 1'}$$

$$\frac{dC_{PER}}{dt} = k_{12} \times C_A - k_{21} \times C_{PER} \qquad \text{Eq. 3'}$$

In both the initial and reduced models, R_0, Q_H, and V_H were treated as constants. V_H was calculated from liver weight assuming a density of liver tissue of approximately 1

g/mL. Q_H was estimated with baseline MDZ concentrations using the following equations for each rat.

$$\text{Metabolic Rate} = Q_H \times (C_A - C_{HV}) \quad \text{Eq. 4}$$

$$Q_H = CL_H / ER \quad \text{Eq. 5}$$

$$CL_H = \text{Dose} / AUC_A \quad \text{Eq. 6}$$

$$ER = (C_A - C_{HV}) / C_A \quad \text{Eq. 7}$$

where CL_H and ER are hepatic clearance and hepatic extraction ratio, respectively. AUC_A is the AUC calculated from aortic concentration-time data.

Plasma MDZ concentrations were converted to blood concentrations based on a blood-to-plasma ratio of 0.7 (Takedomi et al., 2001). The aorta and hepatic vein concentration-time data of MDZ before and after ERY treatments were fitted simultaneously to the base and reduced models (Eq. 1', 2, and 3') for the estimation of V_{max} and K_m. Based on the goodness of fit criteria, the weighted sum of square of residuals (WSS^2) of the reduced model was significantly smaller than that of the base model (WSS^2 = 0.23 ± 0.12 and 1.64 ± 0.95 for reduced and base models, respectively, p<0.05). Therefore, the reduced model was adopted for the estimation of changes in V_{max} and K_m.

***In Vivo* Enzyme Kinetic Analysis**

Based on the predicted aortic and hepatic vein concentration-time profiles of MDZ, the *in vivo* metabolic rates were calculated based on Eq. 4 - 7. The metabolic rates were plotted against the corresponding MDZ concentration in the hepatic vein, which was assumed to be equivalent to MDZ concentration in the hepatocytes, consistent with the assumptions of the well-stirred model (Rowland et al., 1973). The Lineweaver-Burk plot was employed to examine the type of *in vivo* inhibition observed after single and multiple doses of ERY.

Determination of Plasma Concentration of ERY and MDZ

Plasma concentration of ERY, MDZ, and 4-OH MDZ were determined using LC/MS methods as previously described (Lam et al., 2006; Belle et al., 2002).The plasma concentrations of MDZ and 4-OH MDZ were quantified by LC-MS., After the addition of the internal standard (desmethyldiazepam; 30 µL of a 10 µg/mL solution; Sigma Chemical Co, St Louis, MO), and 0.5 mL of a 1 mM sodium hydroxide/glycine buffer (pH 11.3) to 0.5 mL of plasma, the samples were extracted with 3 mL cyclohexane/ethylacetate (50:50, V/V) and the organic layer evaporated to dryness under nitrogen. The dried sample extract was reconstituted with 120 µL of mobile phase (acetonitrile/methanol/10 mM ammonium acetate (pH=7.6), 40:20:40 V/V/V), and 10 µL was injected onto the column (C18 Luna 3 um 2.0 X 100 mm, Phenomenex, Torrance, CA). The column was eluted isocratically with mobile phase at a flow rate of 0.2 mL/min. The effluent was delivered to a mass spectrometer (Navigator; Thermo Finnigan, San Jose, CA). The electrospray ionization probe was run in the positive ion mode with probe temperatures of 400 °C. MDZ and 4-OH MDZ were detected in the selected ion recording mode at m/z 0f 326 and 342, respectively. The limit of quantification in plasma was 200 pg for MDZ and 4-OH MDZ.

Determination of Microsomal Protein Concentration and CYP Complex Formation

Rat livers were weighed and the rat liver microsomes (RLMs) prepared by the method of differential centrifugation (Franklin and Estabrook, 1971). The total microsomal protein concentrations were determined by the method of Lowry (Lowry et al., 1951). The concentration of uncomplexed CYPs, complexed CYPs, and total CYPs were measured independently as previously described (Omura and Sato, 1962; Franklin, 1991). Specifically, for the determination of total CYP, 10 µL of 5 mM potassium ferricyanide was first added to a 1 ml solution containing 1 mg of microsomal protein, 100 mM sodium phosphate buffer (pH=7.4), and 5 mM magnesium chloride to breakdown CYPs that were present as MIC. Following decomplexation, the procedure used for the measurement of free CYPs was followed to obtain total CYP content.

Determination of CYP3A Activity in Rat Liver Microsomes

The CYP3A activity in microsomes from the livers obtained at baseline, after a single dose of ERY, at the end of multiple doses of ERY, and on the days after the discontinuation of ERY was quantified *in vitro* using 4-OH MDZ formation as the probe reaction. Briefly, 0.25 mg microsomal protein was incubated with MDZ at a saturating concentration of 500 µM in sodium phosphate buffer (0.1 M, pH=7.4) with a final incubation volume of 1 mL. NADPH (1 mM final concentration) was added and the microsomes incubated at 37°C for five minutes. The enzyme reaction was terminated by adding 1 mL ice-cold acetonitrile. All experiments were performed in triplicate.

Isolation and Measurement of CYP3A2 mRNA

Total RNA was isolated from rat livers using the RNeasy mini kit (QIAGEN Inc., Valencia, CA) according to the manufacturer's instructions. RNA yield was determined by spectrophotometry (Beckman DU 640; Beckman Coulter, Inc, Fullerton, CA), and quality was assessed by the 260/280 nm ratio. cDNA was synthesized from one gram of total RNA in a 20 µL mixture using random hexamers and avian myeloblastosis virus (AMV) reverse transcriptase (Promega Corp., Madison, WI). A real-time polymerase chain reaction (PCR) method was used to determine the amount of hepatic CYP3A2 mRNA based on a previously described method with minor modifications (Ronis, et al., 2006). Primers specific to CYP3A2 transcripts were purchased from Integrated DNA Technologies (Coralville, Iowa). Rat CYP3A2-specific forward and reverse primers were 5'-TCT CTA CCG ATT GGA ACC CAT AG-3'and 5'-TTG TAG TAA TTC AGC ACA GTG CCT AA-3'. The CYP3A2 expression was normalized to that of the housekeeping gene glyceraldehyde 3-phosphate dehydrogenase (GAPDH). The forward and reverse primers for GAPDH were 5'-TGA TGC TGG TGC TGA GTA TGT CGT-3' and 5'-TTC TCG TGG TTC ACA CCC ATC ACA-3', respectively. Melt-curve analysis was used to ensure that the expected PCR products were being generated

DMD Fast Forward. Published on October 1, 2009 as DOI: 10.1124/dmd.109.028290
This article has not been copyedited and formatted. The final version may differ from this version.

continuously and reproducibly in each real-time PCR reaction. A dilution series (200 femtograms to 0.2 attograms) containing the cDNA for CYP3A2 and GAPDH was applied to generate calibration curves to quantify mRNA normalized to GAPDH expression.

Reversible and Irreversible Inhibition Parameter Estimation for ERY with RLMs

To estimate the reversible inhibition constant K_i, MDZ (10 to 200 µM) and ERY (25 to 300 µM) were incubated with RLMs (0.25 mg) in sodium phosphate buffer (0.1 M, pH 7.4) and NADPH (1 mM) at 37°C for three minutes. The enzyme reaction was terminated by adding 1 mL ice-cold acetonitrile. For the determination of inactivation parameters, RLM (0.25 mg) were preincubated in a 50 µL reaction mixture with ERY at 2.5, 10, 25, 100 µM in the presence of NADPH (1 mM) at 37°C for 0, 1, 2, and 5 minutes. Then 950 µL of incubation mixture containing MDZ and 1 mM NADPH in 0.1 M sodium phosphate buffer were transferred into the preincubation tube (to achieve a final MDZ concentration of 300 µM) and further incubated at 37°C for five minutes.
The reversible inhibition constant K_i was estimated by fitting the appropriate inhibition models (competitive, noncompetitive, or uncompetitive) to the 4-OH MDZ formation rate vs. MDZ concentration data using nonlinear regression (WinNonlin 4.0; Pharsight, Mountain View, CA). Lineweaver-Burk plots were constructed to differentiate modes of inhibition.

To estimate the inactivation constants, the natural logarithm of the percentage of the remaining activity was plotted against preincubation time. The observed inactivation rate constants (k_{obs}) were determined from the slopes of the initial linear decline in activity. The parameters k_{inact} and K_I were obtained from simultaneous fitting of the data of the percentage of the remaining activity vs. the preincubation time at all inhibitor

DMD Fast Forward. Published on October 1, 2009 as DOI: 10.1124/dmd.109.028290
This article has not been copyedited and formatted. The final version may differ from this version.

concentrations using nonlinear regression (WinNonlin 4.0; Pharsight, Mountain View, CA) according to the following equations:

$$\frac{E_t}{E_0} = e^{-k_{obs} \times t} \qquad \text{Eq. 8}$$

$$k_{obs} = \frac{k_{inact} \times I}{K_I + I} \qquad \text{Eq. 9}$$

where E_t and E_0 are enzyme activity at time 0 and t, respectively. k_{obs} is inactivation rate constant, k_{inact} is the rate constant that defines the maximal rate of inactive enzyme formation, I is the initial concentration of the inhibitor, and K_I is the inhibitor concentration when $k_{obs} = k_{inact}/2$.

Prediction of *In Vivo* CYP3A Inhibition by Erythromycin

Prediction using a single inhibitor concentration

A simple algebraic equation was used to predict the fold-decease in CL_{int} of MDZ after multiple doses of ERY treatment as shown in Eq. 10, (Wang et al., 2004).

$$\frac{CL_{int}'}{CL_{int}} = \frac{f_m}{1 + \frac{k_{inact} \times I_u}{k_{deg} \times (K_I + I_u)}} + (1 - f_m) \qquad \text{Eq. 10}$$

where fm is the fraction of the total hepatic elimination that is due to the CYP3A pathway in the absence of the inhibitor. Iu is the unbound inhibitor concentration. A defined value of fm for MDZ could not be obtained from the literature, thus a value of 0.9 was assumed for fm for the prediction based on a study that suggested MDZ was almost "exclusively" metabolized by CYP 3A to form 4-OH MDZ in rats (Shaw et al., 2002). Because MDZ was given three hours into ERY infusion, a time-averaged ERY concentration from 3 to 5.5 hrs after the initiation of ERY infusion was calculated and

considered to best reflect the inhibitor exposure. Fraction of unbound ERY in rat plasma is 0.15 (Lam et al., 2006). The values of enzyme parameters (kinact, KI, and kdeg) used for Eq.10 were the same as those used for the interaction model.

The values of four key model parameters (fm of MDZ, k_{inact} and K_I of ERY, and CYP3A k_{deg}) were varied 10-fold (fm varied from 0.8 to 0.99 to be more realistic for MDZ) within the simulation environment to rank order the importance of their influences on predicting ERY inhibition of MDZ clearance.

Prediction Using a PBPK Approach

To predict the change in the amount of CYP3A in the liver in response to ERY treatment, an interaction model was developed as depicted in Fig 1. A multi-compartment model was developed for ERY based on the reported pharmacokinetic and physiological parameters in rats. In this model, V_C, V_{PER}, and V_H are the volume of central, peripheral, and liver compartment, respectively. k_{12} and k_{21} are the rate constants for distribution between the central and peripheral spaces.

CYP3A enzyme pool in the liver was modeled as a separate compartment (Fig. 1 Enzyme model) based on Eq. 11 (Zhang, et al., 2008)

$$\frac{dE_t}{dt} = k_{deg} \times E_0 - k_{deg} \times E_t - \frac{k_{inact} \times I_{u,t}}{K_I + I_{u,t}} \times E_t \qquad \text{Eq. 11}$$

where E_t and E_0 are enzyme activity at time 0 and t, respectively, k_{deg} is CYP3A degradation rate constant and $I_{u,t}$ is the unbound inhibitor concentration at time t. Following ERY administration, the unbound concentration of ERY in the liver ($I_{u,t}$) together with the inactivation parameters (k_{inact} and K_I) determine the inactivation rate constant, which, in turn, determines the change in the amount of CYP3A in the liver with time.

The parameters used for the ERY model and the enzyme model are listed in Table 1. Simulations were performed using Pharsight Trial Simulator (Pharsight Inc., Mountain View, CA) to predict the time course of ERY and the corresponding change in CYP3A activity under the scenario of ERY 150 mg iv infusion for six hours once a day for four days. The result was compared to the observed ERY concentrations and the decrease in CYP3A activity observed both *in vivo* and *in vitro*.

Results

MDZ aortic and hepatic vein blood concentration-time data were simultaneously fit to a non-linear 2-compartment model depicted in Figure 1 (Drug model). The model provided a good fit to the data obtained in the absence of ERY, after multiple doses of ERY (150 mg by infusion over six hours for four days), and after a single dose of ERY (150 mg infused over 6 hours) (Fig. 2). MDZ concentrations in both the aorta and hepatic vein were elevated after single and multiple dose ERY treatment indicating significant inhibition of MDZ elimination. The difference between the fitted lines of aorta and hepatic vein is equal to the rate of hepatic extraction of midazolam (Eq. 7). The intrinsic clearance (V_{max}/K_m ratio) of MDZ, estimated from the fitting of the blood concentration time data, was reduced by ERY by 1.5 ± 0.7-fold and 2.3 ± 1.4-fold for the single and multiple doses ERY treatment, respectively (Table 2).

Figure 3 shows the relationship between the estimated *in vivo* rates of MDZ metabolism, determined from the post-distributional difference in aortic and hepatic vein blood concentrations (Eq. 4 – 7), and substrate concentration; classical Michaelis-Menten relationships were observed. The *in vivo* V_{max} was reduced from 136.9 to 71.4 µg/min after multiple ERY doses, as reflected in the higher y-intercept in double reciprocal plot (Fig. 3A and B). Single dose ERY did not affect the maximum MDZ metabolic rate but increased the *in vivo* K_m from 1.4 to 3.1 µg/mL; this is reflected in the greater negative x-intercept in the double reciprocal plot (Fig. 3 C and D).

The effect of ERY dosing *in vivo* on the *in vitro* hepatic CYP3A activity, determined as maximal rate of MDZ 4-hydroxylation, is shown in Fig. 4. There was no significant difference in CYP3A concentrations between the control rats and the rats treated with single dose of ERY ($p = 0.06$). However, multiple doses of ERY significantly decreased CYP3A activity (2.1±1.2-fold, $p < 0.01$) when compared with controls.

DMD Fast Forward. Published on October 1, 2009 as DOI: 10.1124/dmd.109.028290
This article has not been copyedited and formatted. The final version may differ from this version.

CYP3A activity recovered gradually after the last dose of ERY and returned to the control values by day three (p=0.4, Fig. 4).

The effect of ERY treatment on the microsomal cytochrome P_{450} (CYP) content is summarized in Table 3. The presence of MIC was not detected in liver microsomes from control rats or rats treated with a single dose of ERY, but was readily detected following multiple doses of ERY. The microsomal MIC content declined upon discontinuation of ERY and had essentially disappeared by three days after the discontinuation of ERY. Table 3 also indicates that the content of uncomplexed CYP was not significantly changed by the treatment with either single or multiple doses of ERY. However, there was a non-statistically significant increase in the total CYP content following multiple doses of ERY (0.49 ± 0.08 vs. 0.71 ± 0.18 nmol/mg protein). Furthermore, as shown in Fig. 4A, the formation of MIC following multiple doses of ERY was coupled with significant decrease ($p < 0.01$) in CYP3A activity and the decline in the content of MIC after the last administration of ERY was accompanied with gradual recovery in CYP3A activity. Based on the slope of the semilogarithmic plot of the time course of the elimination of MIC after the last dose of ERY treatment of four days, the elimination rate constant was estimated to be 0.0349 hr^{-1} (Fig. 4B). This is equivalent to the degradation rate constant, k_{deg}, of CYP3A in rats, and translates into a CYP3A4 half life of 20 hrs.

To examine whether induction occurred after ERY treatment, the relative expression of CYP3A2 mRNA normalized to GAPDH in the liver samples was determined using real-time RT PCR. No significant changes were observed in CYP3A2 at the mRNA level after multiple or single dose of ERY treatments (data not shown).

The potency of ERY as both a mechanism-based inhibitor and a competitive inhibitor of CYP3A was evaluated *in vitro* with the RLMs. Fig. 5A shows time- and

inhibitor concentration-dependant inhibition of CYP3A by ERY. Co-incubation of ERY and MDZ for three minutes resulted in apparent competitive inhibition of CYP3A (Fig. 5B). The estimated values (mean ± sd) for k_{inact}, K_I, and K_i are 0.04 ± 0.02 min^{-1},15.1 ± 3.2 μM, and 117 ± 21μM, respectively. These values were used for the prediction of *in vivo* CYP3A inhibition resulting from ERY treatments.

The inhibition of MDZ intrinsic clearance by ERY was predicted by two methods. The first method incorporated the frequently used assumption of a static, time-averaged inhibitor concentration, as described by Eq. 10. For an assumed fm of MDZ of 0.95, the corresponding prediction was a 15.4-fold decrease I the Clint of MDZ (Table 4). The second method of prediction utilized dynamic inhibitor concentration-time profile for the same ERY multiple dosing regimen employed in our *in vivo* experiments. The predicted ERY concentrations are shown in Fig. 6 (Upper panel) and the corresponding inhibition of hepatic CYP3A, using Eq. 11, is illustrated in Fig. 6 (lower panel). The observed ERY concentrations were determined in blood samples at 3.5, 4.5, and 5.5 hours after the start of ERY infusion. The percentage of baseline CYP3A activity remaining at the time when MDZ was given for the determination of the in vivo CYP3A activity was predicted to be 35% as indicated by the arrow in Fig. 6 (lower panel). The corresponding increase in MDZ AUC is predicted to be 2.6-fold, assuming an fm by CYP3A of 0.95 for MDZ (instantaneous value at the time MDZ was given).. This observation time corresponds to the time when the livers were removed from rats in the second experimental group for the measurement of CYP3A activity *in vitro*.

The influence of each variable on the predicted AUC ratio is shown in Fig. 7. The solid vertical line depicts the mean of AUC ratio, which was predicted using the parameter values listed in Table 4. The horizontal bars depict the range of predicted AUC ratios at parameter values that span a 10-fold range and contain the mean value of

DMD Fast Forward. Published on October 1, 2009 as DOI: 10.1124/dmd.109.028290
This article has not been copyedited and formatted. The final version may differ from this version.

each parameter used in the predictions presented earlier. The most influential variable following the KTZ dosing was the fraction of metabolic clearance attributable to the inhibited pathway (fm). The k_{inact} of ERY and CYP3A degradation rate constant k_{deg} are equally influential within the 10-fold limits.

DMD Fast Forward. Published on October 1, 2009 as DOI: 10.1124/dmd.109.028290
This article has not been copyedited and formatted. The final version may differ from this version.

Discussion

The prediction of *in vivo* DDIs based on *in vitro* CYP inhibition potency is routinely undertaken to understand the drug interaction potential of established drugs and new chemical entities (Clarke and Jeffrey, 2001; Obach et al., 2007; Zhang et al., 2009). However, there is considerable uncertainty in the fidelity of these predictions, especially when MBI is involved. In the current study, we predicted the *in vivo* consequence of MBI following acute and chronic administration using a PBPK model that takes into consideration the temporal change in the inhibitor concentration, the time course of the change in the active CYP3A enzyme pool, and its impact on the disposition of both inhibitor and substrate. We successfully predicted the decrease in the *in vivo* CL_{int} of MDZ after ERY treatment, and demonstrated the utility of trans-hepatic concentration-time data obtained with a rat model to identify the nature of enzyme inhibition kinetics *in vivo*.

Our study design takes advantage of a chronically-cannulated rat model in which the animals are allowed to completely recover from the effects of surgery and anesthesia. Experiments are performed after the animals have returned to non-stressed, physiological baseline after the placement of catheters. In a previous study, the concentration-time curves of MDZ were different in rats studied immediately after regaining the righting reflex and those three days post-surgery; this difference was reflected by a 45% increase in systemic clearance and a 50% decrease in hepatic availability in the chronically-catheterized rats compared to the rats from acute surgery group (Uhing et al., 2004). This acute surgical effect is clearly undesirable yet is often present when the rat is used to study *in vitro-in vivo* extrapolation of drug clearance and to test predictive DDI models. False conclusions regarding the accuracy of such

predictions may be reached if these studies are performed under the acute surgical conditions which can alter the *in vivo* clearance.

In this study, simultaneous sampling of MDZ blood concentrations from the abdominal aorta and hepatic vein enabled us to measure the rate of extraction across the liver at any point in time. For MDZ, a drug exclusively eliminated in the rat liver by CYP3A2-mediated metabolism (Shaw et al, 2002), this extraction rate represents the rate of hepatic metabolism. Our pharmacokinetic analysis assumes the well-stirred model of hepatic elimination and hence, the unbound concentration of MDZ in the hepatic vein (equivalent to the unbound hepatocyte concentration) is the driving force for hepatic elimination (Rowland et al., 1973, Wilkinson, 1987). Consequently we are able to construct *in vivo* analogues of Michaelis-Menten curves that relate the rate of MDZ metabolism to the concentration of MDZ in hepatocyte (Fig. 3). In the presence of an inhibitor, this approach allows the mechanism of inhibition *in vivo* and the potency of the inhibitor to be determined (Fig 3). In this first application of this approach, we characterized the *in vivo* inhibition profile of the well-characterized CYP3A inhibitor, ERY. Our data indicates that in the rat, ERY is a weak competitive inhibitor of CYP3A following a single dose but a modestly potent “apparent noncompetitive” inhibitor following repeated dosing (Fig. 3). This transition from a competitive to an “apparent noncompetitive” mechanism of inhibition is precisely what would be expected for a mechanism-based inhibitor such as ERY. At a given point in time, noncompetitive inhibition and mechanism-based inhibition, both characterized by reduced V_{max}, cannot be distinguished. In our novel approach these mechanism are resolved by the distinct temporal pattern of inhibition observed. This conclusion was consistent with the significant amount of MIC formed in the livers treated with multiple doses of ERY and

lack of MIC formation in the control livers and livers obtained after the treatment with a single dose of ERY (Table 3 and Fig. 4A).

The MDZ concentration-time data obtained from simultaneously sampling from the abdominal aorta and hepatic vein allows the estimation of hepatic intrinsic clearance directly from the *in vivo* V_{max} and K_m values (Rowland et al., 1973, Wilkinson, 1987). The intrinsic clearance estimates provided valuable information on the "true" change in the CYP3A activity *in vivo* and enabled comparison of the extent of change between the *in vivo* and *in vitro* settings. In the current study, following chronic ERY treatment, the intrinsic clearance estimated by simultaneously fitting the aorta and hepatic vein concentration-time data of MDZ was decreased approximately by 2.3-fold (Fig. 2, Table 2); the CYP3A activity in those livers determined *in vitro* by 4-hydroxy MDZ formation was reduced by 2.1-fold (Fig. 4A). These results suggest that the extent of CYP3A inhibition by ERY, independently estimated using the *in vitro* and *in vivo* systems, were in good agreement. Furthermore, there was a 1.5-fold decrease in the *in vivo* intrinsic clearance, but no significant change was measured in the *in vitro*-estimated CYP3A activity following single dose of ERY administration (Table 2, Fig. 4A). This is consistent with the hypothesis that treatment with a single dose of ERY inhibits CYP3A in a competitive manner and exerts no effect on the enzyme activity measured *in vitro*. These data are consistent with previous studies demonstrating that ERY inhibits CYP3A through 2 mechanisms, namely a quasi-irreversible formation of metabolic intermediate complexes (Lindstrom et al., 1993) and by competitive inhibition (Yang et al., 2005). With respect to competitive inhibition by ERY, Yamano *et al.*, demonstrated an increase in MDZ AUC without MIC formation after a bolus injection of ERY 10 mg/kg to rats (Yamano et al., 2000).

Troleandomycin, a macrolide antibiotic and classical inhibitor of CYP3A, is also an inducer of CYP3A2 and CYP3A4 (Watkins et al, 1986). Whether ERY also acts as a CYP3A inducer remains controversial. While several studies reported increase in total CYPs following ERY treatment (Danan et al., 1981; Amacher et al., 1991), no change in total CYPs was observed in other studies (Yamano et al., 2000; Takedomi et al., 2001). It is not clear why this discrepancy exists across different studies. Differences in the dosing regimens and experimental design may play a role. In this study there was a small but insignificant increase in total CYPs and CYP3A2 mRNA after chronic ERY (Table 3). The lack of significant change in CYP3A2 mRNA rules out induction by transcriptional activation but it remains theoretically possible that substrate binding results in induction by protein stabilization, as noted for CYP2E1 (Chien et al., 1997) Although formation of a MIC appears to stabilize CYP3A in vivo and result in an increase in immunoquantifiable protein there is no increase in activity because the accumulating complex is inactive (Larrey et al.,1983). There is no evidence to support induction of active CYP3A by mechanisms other than transcriptional activation and therefore in our model the effects of ERY are restricted to reversible and irreversible inhibition.

Our 4-day dosing regimen resulted in the *in vivo* formation of MIC that was easily quantified spectrophotometrically (Fig. 4A). Following discontinuation of ERY dosing, the amount of MIC present in the liver declined in a first-order manner with an estimated elimination rate constant of 0.035 hr^{-1} (Fig. 4B) assuming a zero order rate for CYP3A synthesis that is unaffected by ERY administration and a first-order rate of enzyme degradation. Our estimate is within the range of CYP3A elimination rate constants in rats (0.0348-0.072 hr^{-1}) estimated in previous studies (Shiraki and Guengerich, 1984; Correia, 1991). An accurate estimation of the degradation rate constant is critical for the prediction of the extent and time course of irreversible inhibition *in vivo* (Mayhew et al.,

2000; Zhang, et al., 2009; Zhang, et al., 2009). As demonstrated by the sensitivity analysis, a 10-fold variation in k_{deg} resulted in a MDZ AUC ratio change from 8.3 to 18.8. However, this parameter is generally not obtained and this contributes to the poor performance and uncertainty of previous PBPK predictive models of irreversible inhibition *in vivo*.

To test whether the observed decrease in the *in vivo* CL_{int} of MDZ can be predicted using *in vitro*-estimated inactivation parameters, k_{inact} and K_I were estimated in RLMs from livers of rats in the control group. A physiologically-based approach, taking into account the temporal disposition of the inhibitor and the change in the active enzyme pool in the liver, was applied. Conventionally, simple algebraic calculations at a single inhibitor concentration (usually C_{max}) have been commonly adopted, ignoring the changing concentrations of the inhibitor following its administration (Thummel and Wilkinson, 1998; Mayhew et al., 2000; Bjornsson et al., 2003; Wang et al., 2004; Obach et al., 2005). This leads to false prediction in the inhibition potential. To test whether a simplistic equation with one inhibitor concentration is sufficient to predict the interaction between ERY and MDZ, a well-defined equation for the prediction of the extent of MBI (Eq. 10) adapted from a study by Wang and colleagues, was used (Wang, et al., 2004). In the application of Eq. 10, the parameter values were equivalent to those used in the PBPK model, except for a constant single inhibitor concentration, calculated from the time-averaged ERY concentration during the time interval when MDZ was administered. As shown in Table 4, using a time-averaged ERY concentration significantly overestimates the magnitude of the decrease in MDZ CL_{int} (15.4-fold vs. observed 2.3-fold). In contrast, the PBPK model applied in the current study predicted a 2.6-fold decrease in CYP3A activity following repeated ERY treatment, which is in excellent agreement with the observed *in vivo* CL_{int} ratio (2.3-fold, Table 2) and the fold decrease

in the *in vitro*-estimated CYP3A activity (2.1-fold, Fig. 4A). These results suggest both the feasibility and meaningfulness of the physiological prediction strategy applied for the prediction of MBI and confirmed the importance of incorporating the temporal disposition of inhibitor into the prediction.

To summarize, single and multiple dose treatments of ERY resulted in significant reduction in the CL_{int} of MDZ in rats through reversible and irreversible inhibition of CYP3A, respectively. CYP3A inactivation by ERY is mediated through MIC formation without significant changes in the CYP3A2 mRNA. Additionally, the physiologically stable, chronically-cannulated rat model proved to be a valuable tool for the study of the changes in *in vivo* enzyme kinetics. Finally, the PBPK model using *in vitro*-estimated CYP3A inhibition parameters successfully predicted the decrease in MDZ CL_{int} following chronic administration of ERY. Overall, the current work has demonstrated the utility and feasibility of a physiological approach for the prediction of *in vivo* DDIs involving MBI using *in vitro*-estimated enzyme inhibition parameters. This *in vitro-in vivo* extrapolation approach may be applicable to the prediction of possible clinical DDIs in humans.

References

Amacher DE, Schomaker SJ and Retsema JA (1991) Comparison of the effects of the new azalide antibiotic, azithromycin, and ERY estolate on rat liver cytochrome P-450. *Antimicrob Agents Chemother* 35:1186-1190.

Belle DJ, Callaghan JT, Gorski JC, Maya JF, Mousa O, Wrighton SA, and Hall SD (2002) The effects of an oral contraceptive containing ethinyloestradiol and norgestrel on CYP3A activity. *Br J Clin Pharmacol.* 53:67-74.

Bjornsson TD, Callaghan JT, Einolf HJ, Fischer V, Gan L, Grimm S, Kao J, King SP, Miwa G, Ni L, Kumar G, McLeod J, Obach SR, Roberts S, Roe A, Shah A, Snikeris F, Sullivan JT, Tweedie D, Vega JM, Walsh J and Wrighton SA (2003) The conduct of *in vitro* and *in vivo* drug-drug interaction studies: a PhRMA perspective. *J Clin Pharmacol* 43:443-469.

Clarke SE and Jeffrey P (2001) Utility of metabolic stability screening: comparison of in vitro and *in vivo* clearance. *Xenobiotica* 31:591-598.

Correia MA (1991) Cytochrome P450 turnover. *Methods Enzymol* 206:315-325.

Danan G, Descatoire V and Pessayre D (1981) Self-induction by ERY of its own transformation into a metabolite forming an inactive complex with reduced cytochrome P-450. *J Pharmacol Exp Ther* 218:509-514.

Franke RM, Baker SD, Mathijssen RH, Schuetz EG, and Sparreboom A (2008) Influence of solute carriers on the pharmacokinetics oof CYP3A4 probes. *Clin Pharmacol Ther* 84(6):704-9.

Franklin MR (1991) Cytochrome P450 metabolic intermediate complexes from macrolide antibiotics and related compounds. *Methods Enzymol* 206:559-573.

Franklin MR and Estabrook RW (1971) On the inhibitory action of mersalyl on microsomal drug oxidation: a rigid organization of the electron transport chain. *Arch Biochem Biophys* 143:318-329.

Ito K, Ogihara K, Kanamitsu S and Itoh T (2003) Prediction of the *in vivo* interaction between MDZ and macrolides based on in vitro studies using human liver microsomes. *Drug Metab Dispos* 31:945-954.

Chien JY, Thummel KE, and Slattery JT (1997) Pharmacokinetic Consequences of Induction of CYP2E1 by Ligand Stabilization. *Drug Metab Dispos* 25:1165-1175.

Kaminsky LS and Fasco MJ (1991) Small intestinal cytochromes P450. *Crit Rev Toxicol* 21:407-422.

Lam JL, Okochi H, Huang Y, and Benet LZ. (2006) In vitro and *in vivo* correlation of hepatic transporter effects on ERY metabolism: characterizing the importance of transporter-enzyme interplay. *Drug Metab Dispos* 34:1336-44.

Larrey D, Funck-Brentano C, Breil P, Vitaux J, Theodore C, Babany G (1983) Effects of erythromycin on hepatic drug-metabolizing enzymes in humans. *Biochem Pharmacol.* **32**:1063–8.

Lindstrom T, Hanssen B and Wrighton S (1993) Cytochrome P-450 complex formation by dirithromycin and other macrolides in rat and human livers. *Antimicrobial Agents Chemother* 37:265-269.

Lowry OH, Rosebrough NJ, Farr AL and Randall RJ (1951) Protein measurement with the Folin phenol reagent. *J Biol Chem* 193:265-275.

Mayhew BS, Jones DR and Hall SD (2000) An in vitro model for predicting *in vivo* inhibition of cytochrome P450 3A4 by metabolic intermediate complex formation. *Drug Metab Dispos* 28:1031-1037.

Obach RS, Walsky RL and Venkatakrishnan K (2007) Mechanism-based inactivation of human cytochrome p450 enzymes and the prediction of drug-drug interactions. *Drug Metab Dispos* 35:246-255.

Obach RS, Walsky RL, Venkatakrishnan K, Gaman EA, Houston JB and Tremaine LM (2006) The utility of in vitro cytochrome P450 inhibition data in the prediction of drug-drug interactions. *J Pharmacol Exp Ther* 316:336-348.

Obach RS, Walsky RL, Venkatakrishnan K, Houston JB and Tremaine LM (2005) In vitro cytochrome P450 inhibition data and the prediction of drug-drug interactions: qualitative relationships, quantitative predictions, and the rank-order approach. *Clin Pharmacol Ther* 78:582-592.

Omura T and Sato R (1962) A new cytochrome in liver microsomes. *J Biol Chem* 237:1375-1376.

Paine MF, Hart HL, Ludington SS, Haining RL, Rettie AE and Zeldin DC (2006) The human intestinal cytochrome P450 "pie". *Drug Metab Dispos* 34:880-886.

Pershing LK, Franklin, MR: Cytochrome P-450 metabolic-intermediate complex formation and induction by macrolide antibiotics; a new class of agents. Xenobiotica 12: 687-699, 1982

Quinney SK, Galinsky RE, Jiyamapa-Serna VA, Chen Y, Hamman MA, Hall SD and Kimura RE: Hydroxyitraconazole, formed during intestinal first-pass metabolism of itraconazole, controls the time course of hepatic CYP3A inhibition and the bioavailability of itraconazole in rats (2008) *Drug Metab. Dispos.*36:1097-1101

Ronis MJ, Chen Y, Badeaux J, Llaurenzana E, and Badger T (2006) Soy Protein Isolate Induces CYP3A1 and CYP3A2 in Prepubertal Rats. *Exp Bioy and Med* 231:60-69.

Rowland M, Benet LZ and Graham GG (1973) Clearance concepts in pharmacokinetics. *J Pharmacokinet Biopharm* 1:123-136.

Schwenk M (1988) Mucosal biotransformation. *Toxicol Pathol* 16:138-146.

Segel IR (1993) *Enzyme Kinetics*. John Wiley & Sons, INC., New York, New York.

Shaw AA, Hall SD, Franklin MR, and Galinsky RE (2002) The influence of L-glutamine on the depression of hepatic cytochrome P450 activity in male rats caused by total parenteral nutrition. *Drug Metab Dispos* 30:177–182.

Shiraki H and Guengerich FP (1984) Turnover of membrane proteins: kinetics of induction and degradation of seven forms of rat liver microsomal cytochrome P-450, NADPH-cytochrome P-450 reductase, and epoxide hydrolase. *Arch Biochem Biophys* 235:86-96.

Takedomi S, Matsuo H, Yamano K, Ohtani H and Sawada Y (2001) In-vivo kinetics of the interaction between MDZ and ERY in rats, taking account of metabolic intermediate complex formation. *J Pharm Pharmacol* 53:643-651.

Thummel KE and Wilkinson GR (1998) In vitro and *in vivo* drug interactions involving human CYP3A. *Annu Rev Pharmacol Toxicol* 38:389-430.

Thummel KE, O'Shea D, Paine MF, Shen DD, Kunze KL, Perkins JD and Wilkinson GR (1996) Oral first-pass elimination of MDZ involves both gastrointestinal and hepatic CYP3A-mediated metabolism. *Clin Pharmacol Ther* 59:491-502.

Uhing MR, Beno DW, Jiyamapa-Serna VA, Chen Y, Galinsky RE, Hall SD and Kimura RE (2004) The effect of anesthesia and surgery on CYP3A activity in rats. *Drug Metab Dispos* 32:1325-1330.

von Moltke LL, Greenblatt DJ, Schmider J, Wright CE, Harmatz JS and Shader RI (1998) *In vitro* approaches to predicting drug interactions *in vivo*. *Biochem Pharmacol* 55:113-122.

Wang YH, Jones DR and Hall SD (2004) Prediction of cytochrome P450 3A inhibition by verapamil enantiomers and their metabolites. *Drug Metab Dispos* 32:259-266.

Watkins PB, Wrighton SA, Schuetz EG, Maurel P and Guselian PS (1986) Macrolide antibiotics inhibit the degradation of the glucocorticoid-responsive cytochrome P-450p in rat hepatocytes in vivo and in primary monolayer culture. *J. Biol. Chem*. 261:6264-6271.

Wilkinson GR (1987) Clearance approaches in pharmacology. *Pharmacol Rev* 39:1-47.

Yamano K, Yamamoto K, Kotaki H, Takedomi S, Matsuo H, Sawada Y and Iga T (2000) Quantitative prediction of metabolic inhibition of MDZ by ERY, diltiazem, and verapamil in rats: implication of concentrative uptake of inhibitors into liver. *J Pharmacol Exp Ther* 292:1118-1126.

Zhang X, Jones DR, and Hall SD (2008) Mechanism-based inhibition of human cytochromes P450: in vitro kinetics and in vitro-in vivo correlations. In: Drug-drug Interactions, Second Edition. Ed. Rodrigues AS. Marcel Dekker, New York, NY, 2008.

Zhang X, Quinney SK, Gorski JC, Jones DR, and Hall SD (2009) Semi-physiologically-based pharmacokinetic models for the inhibition of midazolam clearance by diltiazem and its major metabolite. *Drug Metab Dispos* 37:1587-1597.

Zhou S, Chan E, Lim LY, Boelsterli UA, Li SC, Wang J, Zhang Q, Huang M and Xu A (2004) Therapeutic drugs that behave as mechanism-based inhibitors of cytochrome P450 3A4. *Curr Drug Metab* 5:415-442.

Footnotes

[1] current affiliation: Department of Drug Disposition, Eli Lilly and Company, Indianapolis, IN

[2] current affiliation: Division of Biostatistics, Indiana University School of Medicine, Indianapolis, IN

Figure legends

Figure 1. The physiologically-based interaction model for the inhibition of the enzyme in the liver by ERY. V_C, V_{PER}, and V_H are the volume of central, peripheral, and liver compartment, respectively. k_{12} and k_{21} are the rate constants for distribution between the central and peripheral spaces. Q_H is liver blood flow. E_t is the amount of enzyme at time t. k_{deg} is CYP3A degradation rate constant and $I_{t,u}$ is the unbound inhibitor (ERY) concentration at time t. k_{inact} and K_I are the rate constant that defines the maximal rate of inactive enzyme formation and the inhibitor concentration to reach half maximal inactivation, respectively. The drug model applies to both the substrate (MDZ) and the inhibitor (ERY).

Figure 2. Plasma concentrations of MDZ in rats following intravenous infusion of 5 mg/kg, In panels A, B and C, open symbols (○) and closed symbols (●) represent observed hepatic vein and aorta concentrations, respectively. Lines are model predicted MDZ hepatic vein (dashed lines) and aorta (solid lines) concentrations, respectively. Panel A shows the time course of MDZ in control rats (n=9). Panel B and C show the time course of MDZ in rats receiving multiple or single doses of ERY, respectively. Panel D shows the time course of MDZ concentrations in aorta (filled symbols) and hepatic vein (open symbols) before (circles) and after (triangles) a single dose of ERY in a representative animal.

Figure 3. The relationship between the estimated *in vivo* hepatic metabolic rate of MDZ (Eq. 4) and the corresponding MDZ blood concentrations in the hepatic vein in the control (open symbols) and after multiple infusions (A) and single infusion (C) of ERY

treatment (closed symbols). The corresponding double-reciprocal plots of the data are represented in panels B and D. The lines represent the best fit to Eq. 4 (panel A and C) and the double reciprocal transformation of Eq. 4 (panel B and D).

Figure 4. The *in vivo*-formed MIC in the livers dissected at various time points before and after ERY treatments (white bars) with corresponding CYP3A activity measured *in vitro* using MDZ as a substrate (diamond) (Panel A). The x-axis represents measurements in the control group (control), at 3h into the 4^{th} dose of ERY (Multiple ERY), on day 1(Day 1), day 2 (Day 2), day 3 (Day 3) after the discontinuation of ERY, and after the single dose ERY treatment (single ERY), respectively. The bar plot uses the y-axis on the left side and the symbols with error bars uses the y-axis on the right side. The *p*-value is for the comparison of CYP 3A activity with baseline. Error bars indicate standard deviation. Panel B shows the time course of the elimination of MIC after the last dose of multiple ERY treatment (B). The elimination rate constant was estimated as -0.035 hr^{-1} (CYP3A half life of 20 hrs).

Figure 5. Time- and ERY concentration-dependant inhibition of CYP3A by ERY (A) and Lineweaver-Burk plot of 4-hydroxyl MDZ (B) after preincubation of ERY at several concentrations in RLMs made from control rats.

Figure 6. Prediction of the inhibition of CYP3A in the liver by multiple doses of ERY treatment using the PBPK model. The upper panel shows the predicted (solid line) and observed (mean ± sd, closed circle) ERY concentrations after ERY treatment (150 mg infusion over six hours, once a day for four days). The lower panel shows the predicted (dashed line) and observed (mean ± sd, open circle) time course of the change in

CYP3A level in response to ERY treatment. The arrow indicates a predicted 35% remaining CYP3A activity at the time MDZ was given to determine the *in vivo* CL_{int} of MDZ.

Figure 7. Model parameter sensitivity for the ERY/MDZ interaction. The four variables, MDZ fm, ERY K_{inact} and K_I, and CYP3A k_{deg}, are allowed to vary over a 10-fold range (except for fm for better illustration) for calculation of the AUC ratios: fm from 0.8 to 0.99, k_{inact} from 0.48 to 72 h-1, CYP3A k_{deg} from 0.006 to 0.15 h-1, and K_I from 3 to 75. The horizontal bars depict the AUC ratio at the lower value and the higher value. The solid vertical lines are mean predicted AUC ratio using the mean values of the variables from Tables 4.

DMD Fast Forward. Published on October 1, 2009 as DOI: 10.1124/dmd.109.028290
This article has not been copyedited and formatted. The final version may differ from this version.

Table 1. Model parameters for ERY and CYP3A used in the simulation.

Parameters		Values	References
PK parameters	V_C (mL)	200	(Yamano et al., 2000)
	V_{PER} (mL)	400	
	CL_R (L/h)	0.05	
	CL_{int} (L/h)	0.54	
	f_u	0.15	(Lam et al., 2006)
Physiological parameters	Q_H (mL/min)	22*	
	V_H (mL)	10*	
	k_{deg} (hr^{-1})	0.0348	Current study
Enzyme inhibition parameters	K_i (μM)	117	
	k_{inact} (min^{-1})	0.04	
	K_I (μM)	15.1	

*Q_H and V_H were calculated for individual rat as described in the text under "The MDZ PK Model". The mean values were used for the simulation.

DMD Fast Forward. Published on October 1, 2009 as DOI: 10.1124/dmd.109.028290
This article has not been copyedited and formatted. The final version may differ from this version.

Table 2. Estimated parameters from fitting the MDZ PK model.

	Control (n=12)	Multiple-dose ERY (n=12)	Control (n=3)	Single-dose ERY (n=3)
V_{max} (mg/mL/min)	142 ± 54	70.8 ± 31.3	130.6 ± 33.4	129.8 ± 35.9
K_m (mg/mL)	1.3 ± 0.4	1.3 ± 0.6	1.5 ± 1.3	1.9 ± 1.5
k_{12} (min^{-1})*	0.09 ± 0.04		0.09 ± 0.04	
k_{21} (min^{-1})*	0.08 ± 0.03		0.10 ± 0.05	
V_C (mL)*	295.1 ± 49.3		217.3 ± 58.1	
V_{max}/K_m (mL/min)	112.8 ± 31.7	53.4 ± 37.3	126.6 ± 64.6	90.4 ± 65.3
Fold decrease in V_{max}/K_m	2.3 ± 1.4		1.5 ± 0.7	
p value[#]	< 0.01		0.06	

Values are presented as mean ± SD.

* k_{12}, k_{21}, and V_c were assumed the same for the simultaneous fitting of MDZ concentrations before and after ERY treatment assuming ERY has no effect on these parameters.

[#] *p* value was calculated for V_{max}/K_m.

DMD Fast Forward. Published on October 1, 2009 as DOI: 10.1124/dmd.109.028290
This article has not been copyedited and formatted. The final version may differ from this version.

Table 3. Effect of multiple and single dose of ERY treatment on uncomplexed CYP, complexed CYP, and total CYP protein content.

	Uncomplexed CYP (nmol/mg protein)	Complexed CYP (nmol/mg protein)	Total CYP (nmol/mg protein)	*p* Value[#]
Control	0.45 ± 0.08	N.D.*	0.49 ± 0.08	NA
Multiple dose of ERY	0.42 ± 0.07	0.31 ± 0.11	0.71 ± 0.18	0.18
1 day after	0.47 ± 0.08	0.17 ± 0.07	0.67 ± 0.11	0.13
2 days after	0.57 ± 0.29	0.09 ± 0.13	0.75 ± 0.38	0.15
3 days after	0.46 ± 0.04	0.05 ± 0.03	0.58 ± 0.03	0.21
Single dose of ERY	0.49 ± 0.03	N.D.*	0.52 ± 0.03	0.32

Values are presented as mean ± SD.

* N.D. Not detected.

[#] *p* Value was calculated for total CYP. NA: not applicable.

DMD Fast Forward. Published on October 1, 2009 as DOI: 10.1124/dmd.109.028290
This article has not been copyedited and formatted. The final version may differ from this version.

Table 4. Parameter values used and the result for the prediction of the decrease in MDZ CL_{int} using single point estimate (Eq. 10).

Parameters	Values
f_m of MDZ	0.95
Mean time-averaged ERY concentration (μM)	54.5
f_u of ERY	0.15
k_{inact} (min^{-1})	0.04
K_I (μM)	15.1
k_{deg} (hr^{-1})	0.03
Prediction results	
Predicted MDZ CL_{int}'/CL_{int}	0.075
Predicted fold-decrease in MDZ exposure	15.4

Figure 1

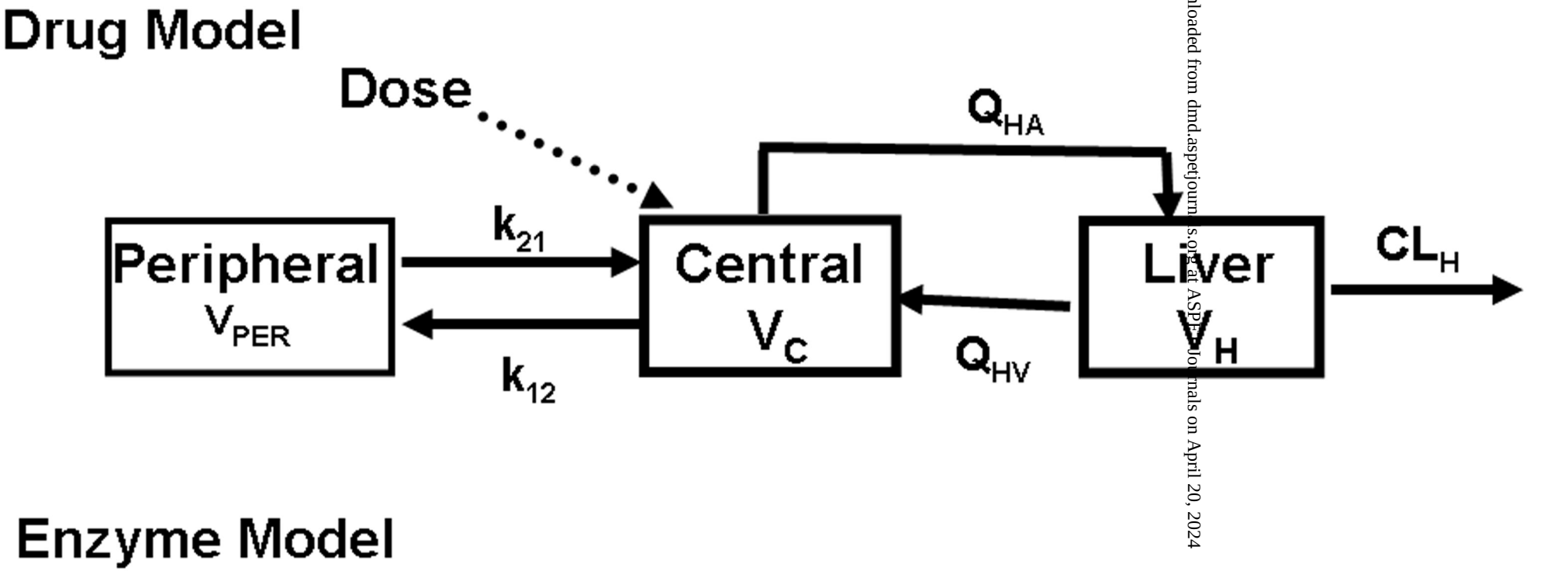

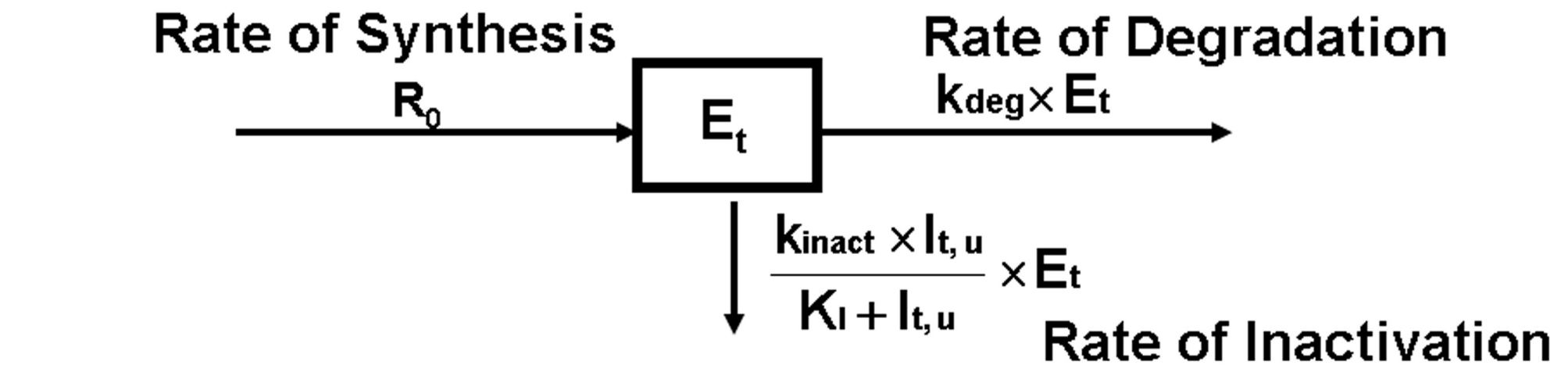

Fig. 2

A

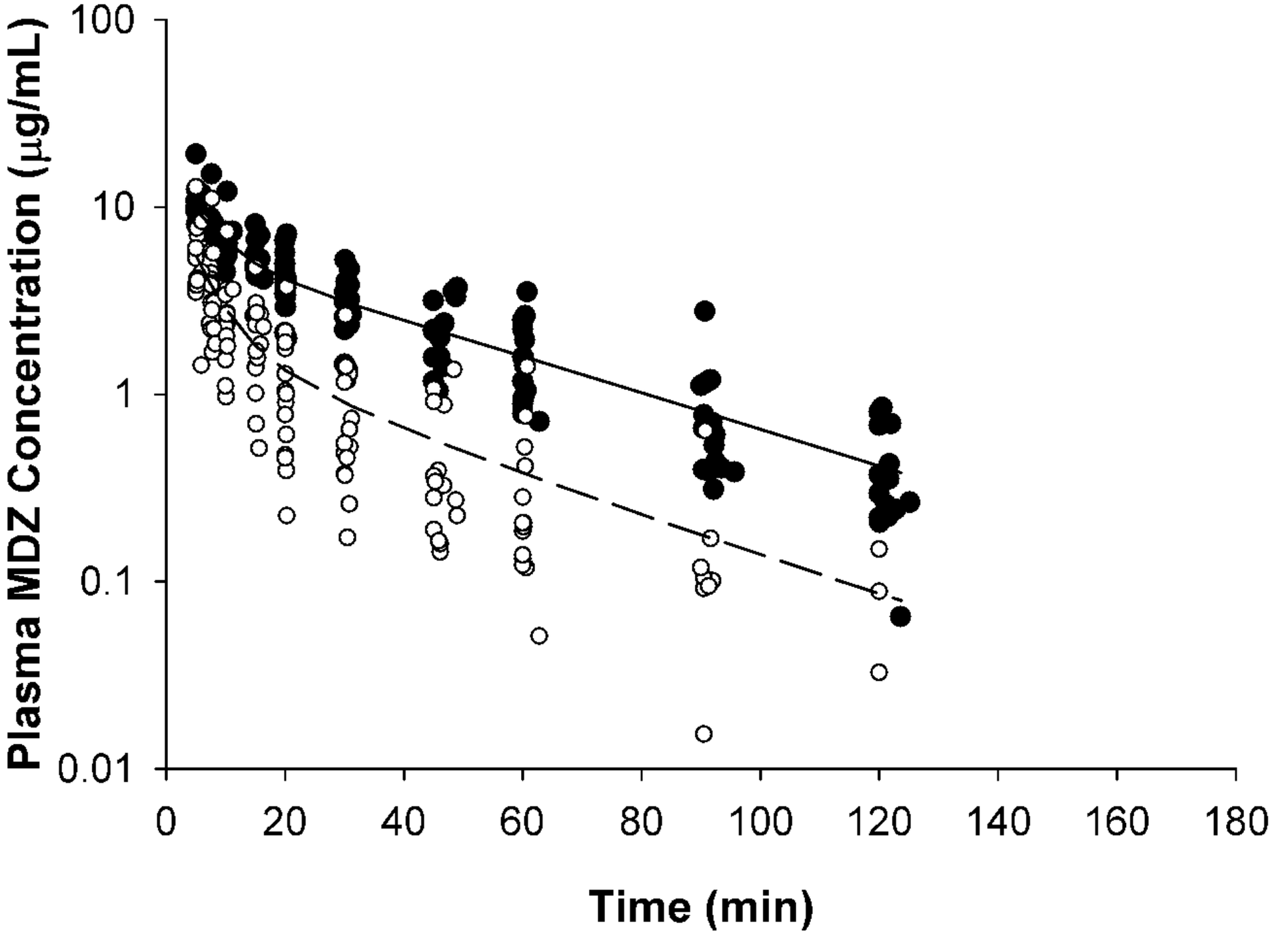
Plasma MDZ Concentration (μg/mL)
100
10
1
0.1
0.01
0
20
40
60
80
100
120
140
160
180
Time (min)

Fig. 2

B

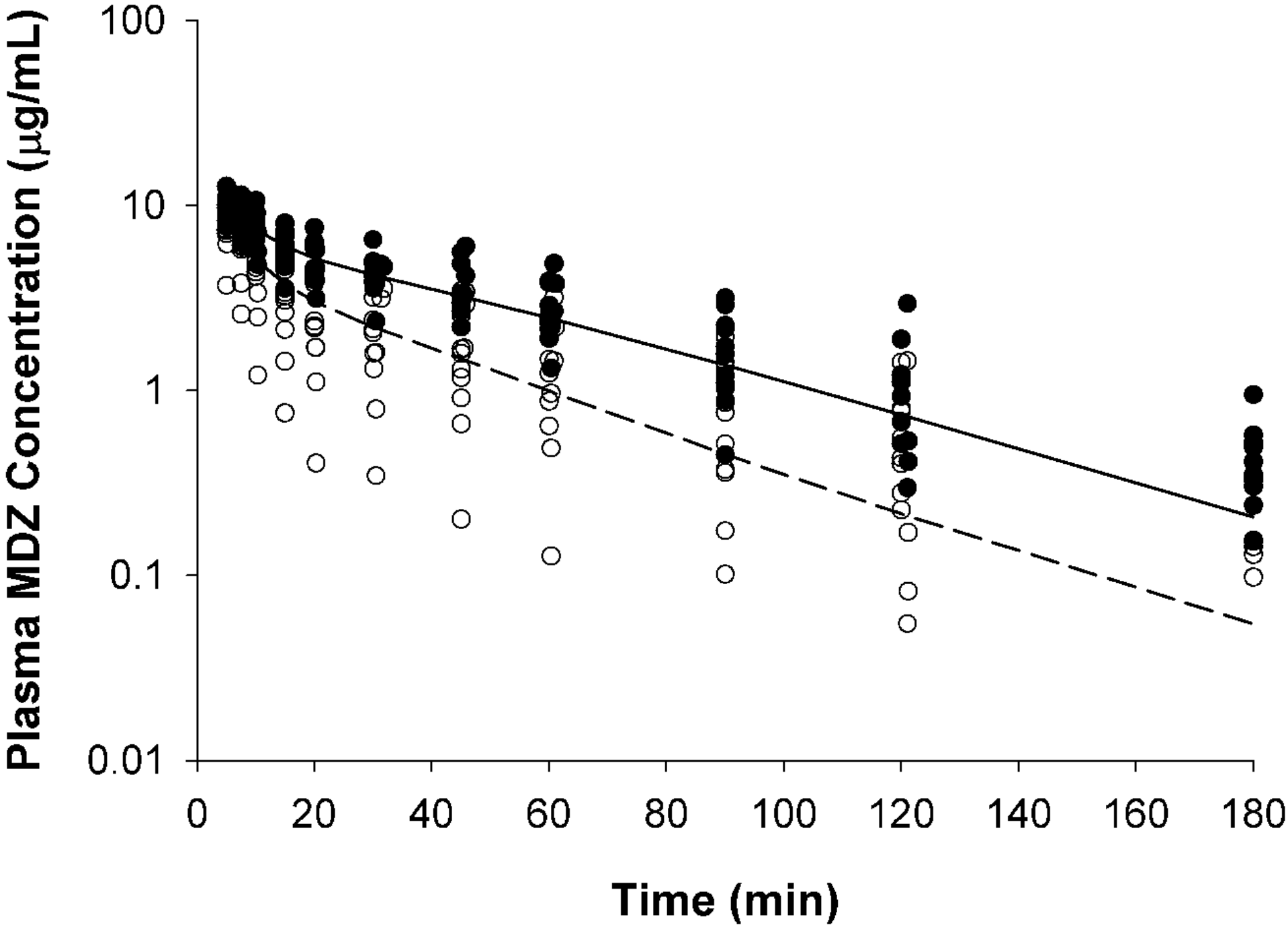
Plasma MDZ Concentration (μg/mL)
100
10
1
0.1
0.01
0
20
40
60
80
100
120
140
160
180
Time (min)

Fig 2

C

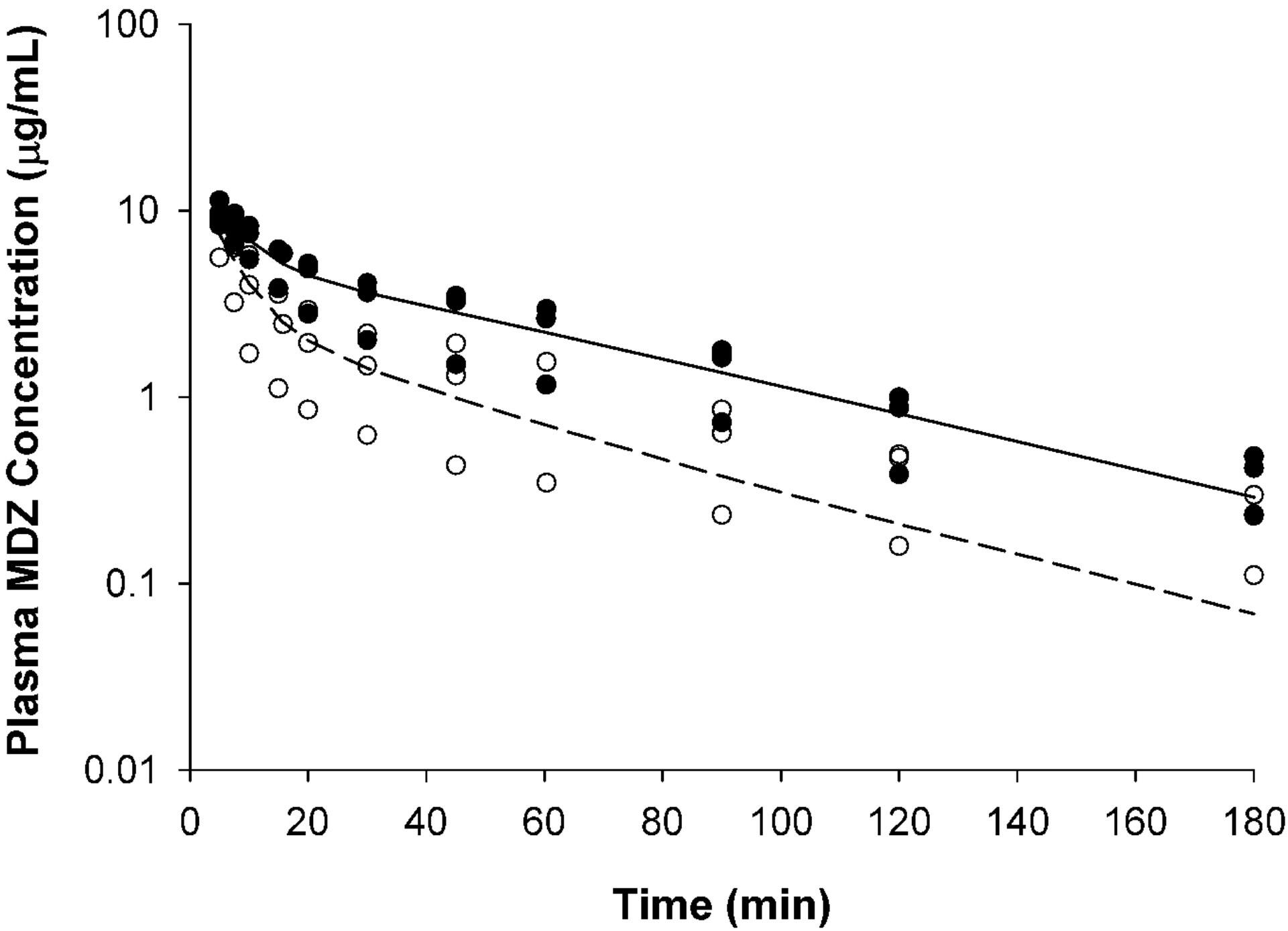
Plasma MDZ Concentration (μg/mL)
100
10
1
0.1
0.01
0
20
40
60
80
100
120
140
160
180
Time (min)

Fig 2

D

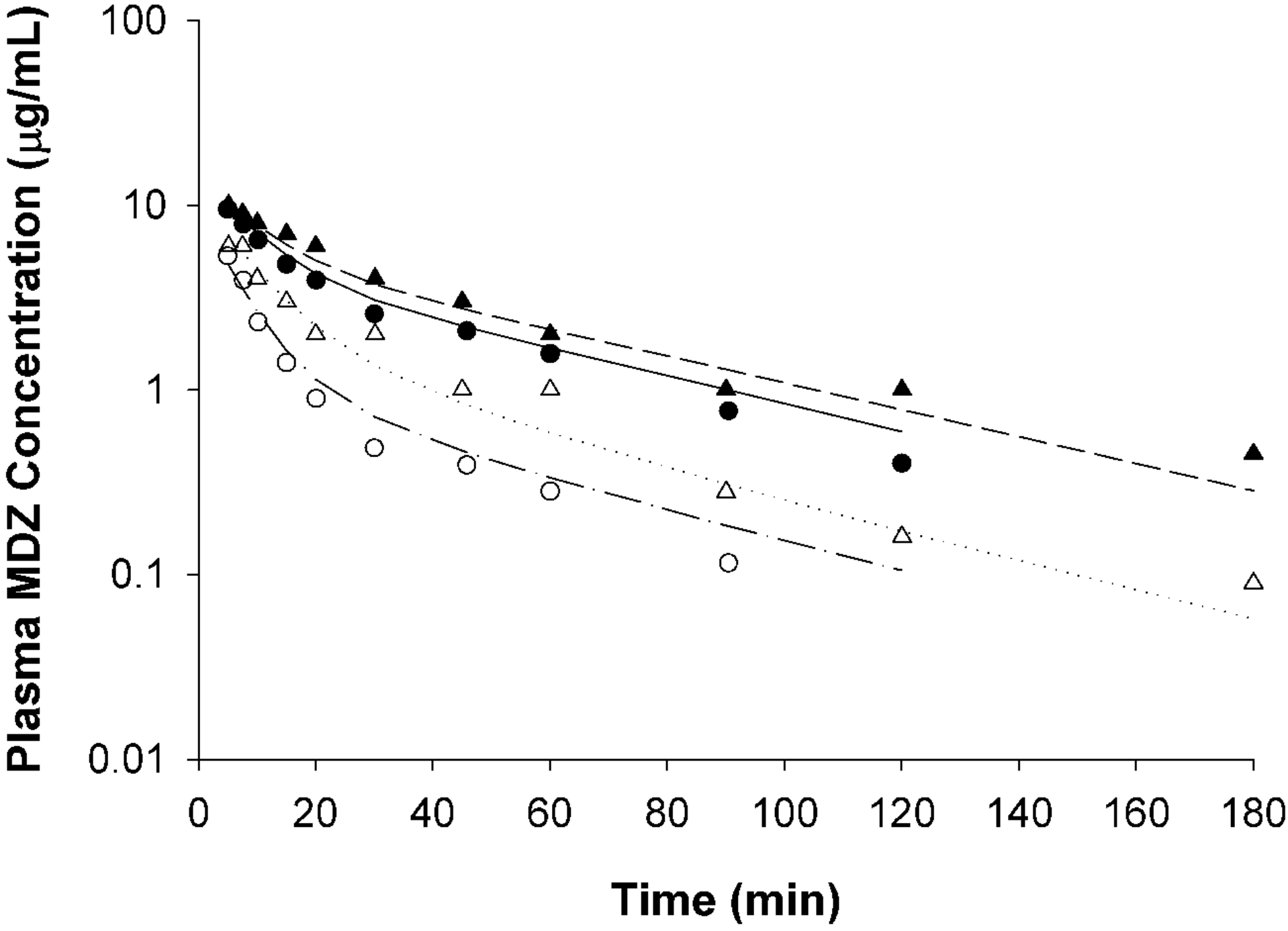
Plasma MDZ Concentration (µg/mL)
100
10
1
0.1
0.01
0
20
40
60
80
100
120
140
160
180
Time (min)

Figure 3

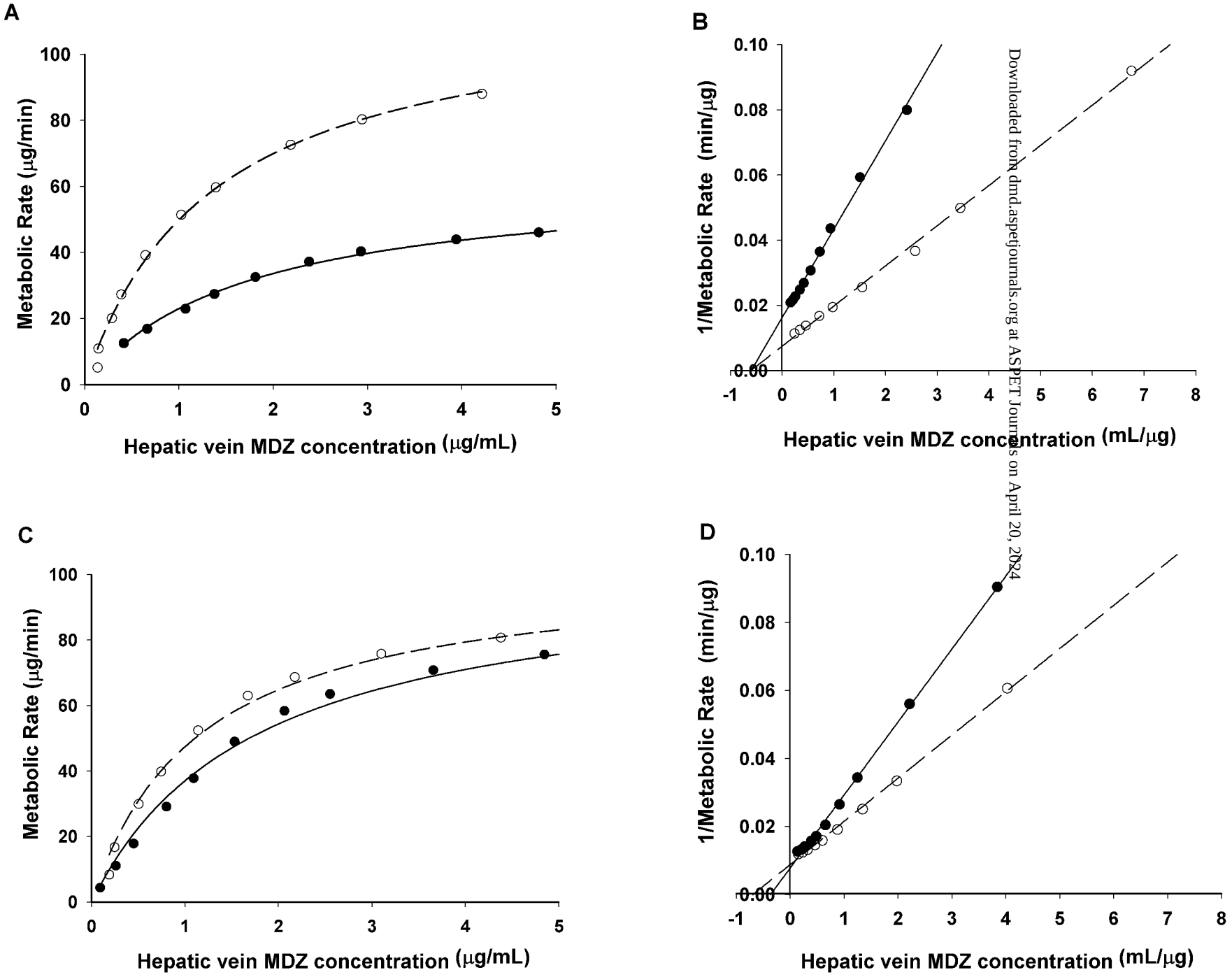

DMD Fast Forward. Published on October 1, 2009 as DOI: 10.1124/dmd.109.028290
This article has not been copyedited and formatted. The final version may differ from this version.

Fig 4
A

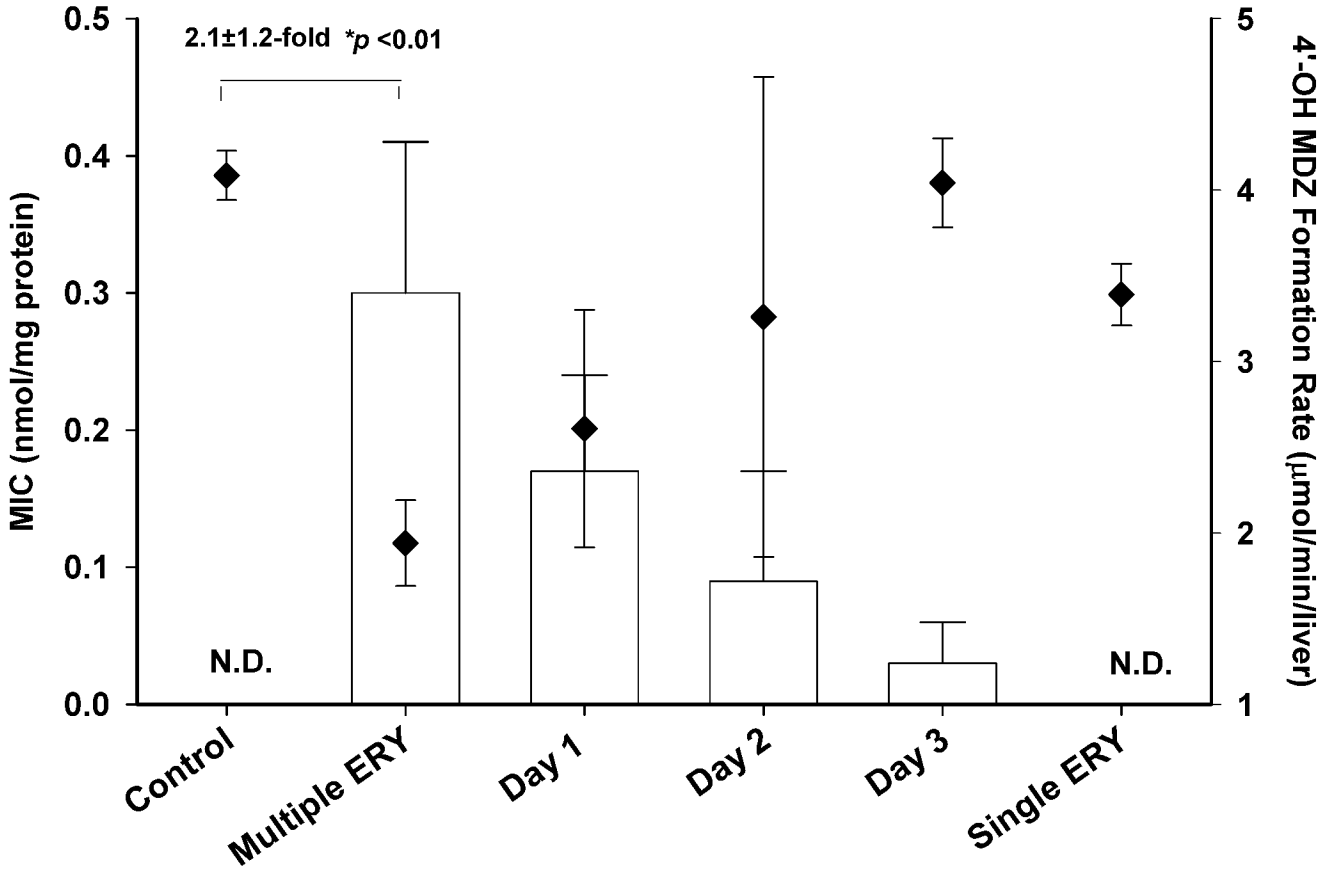

DMD Fast Forward. Published on October 1, 2009 as DOI: 10.1124/dmd.109.028290
This article has not been copyedited and formatted. The final version may differ from this version.

Fig 4

B

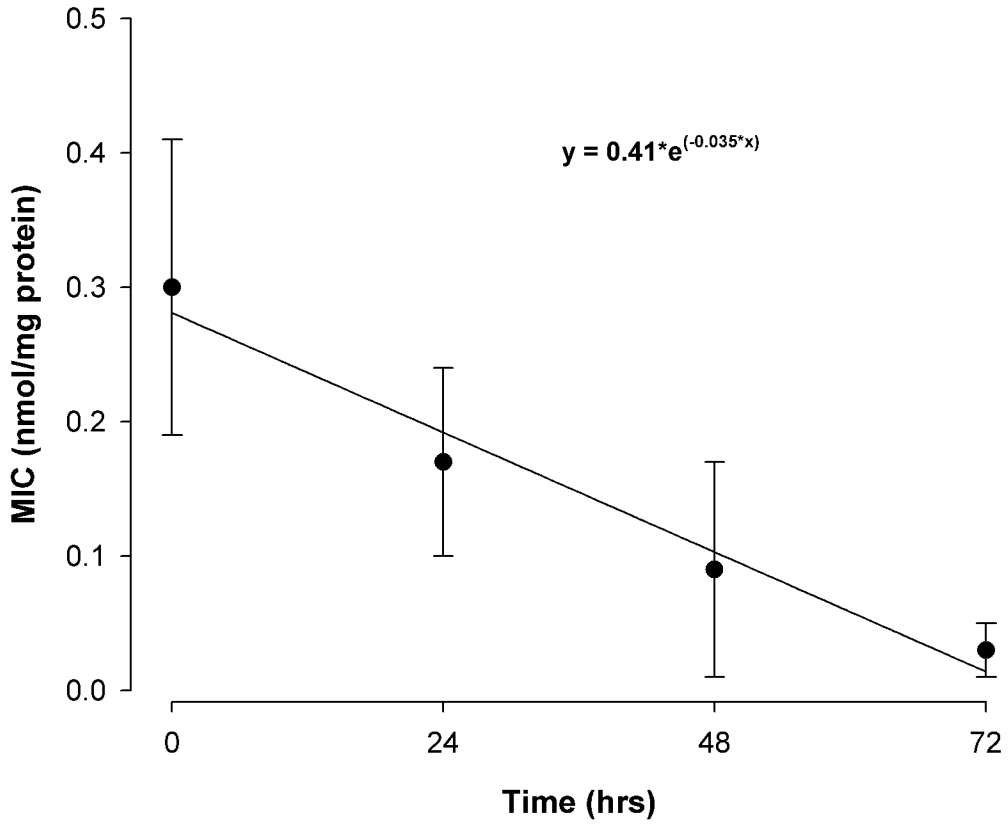

Figure 5
A

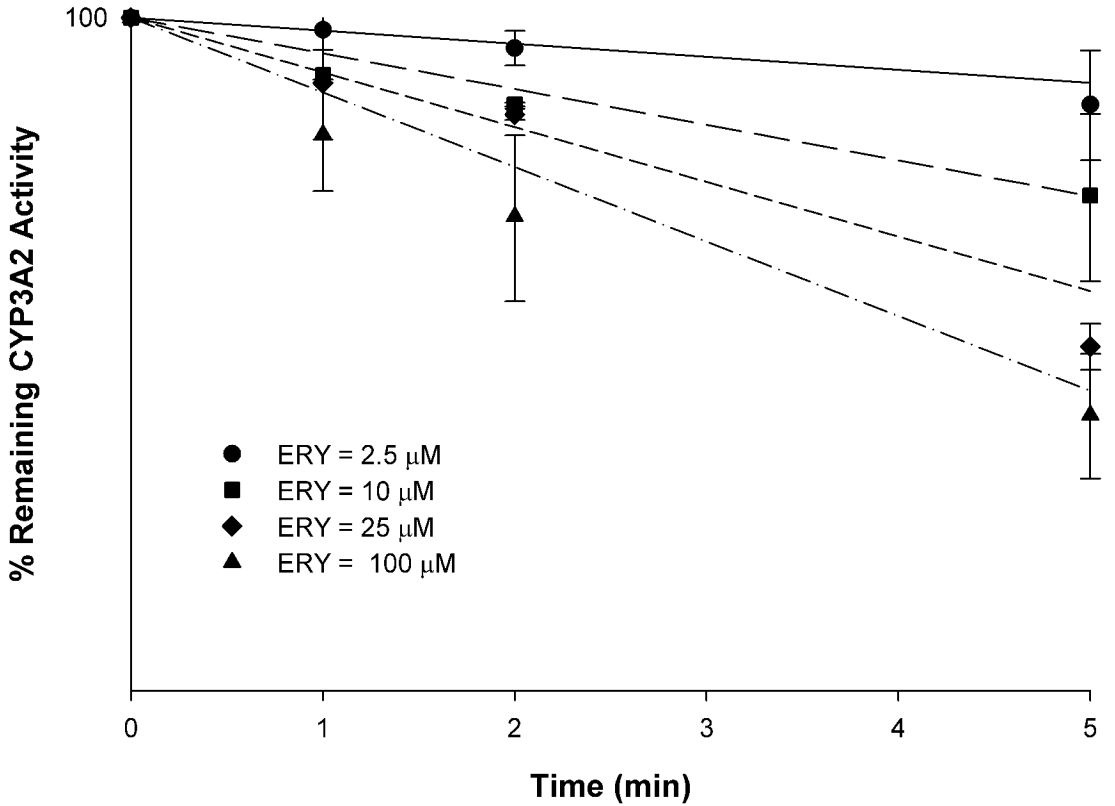
100
% Remaining CYP3A2 Activity
ERY = 2.5 μM
ERY = 10 μM
ERY = 25 μM
ERY = 100 μM
0
1
2
3
4
5
Time (min)

Figure 5
B

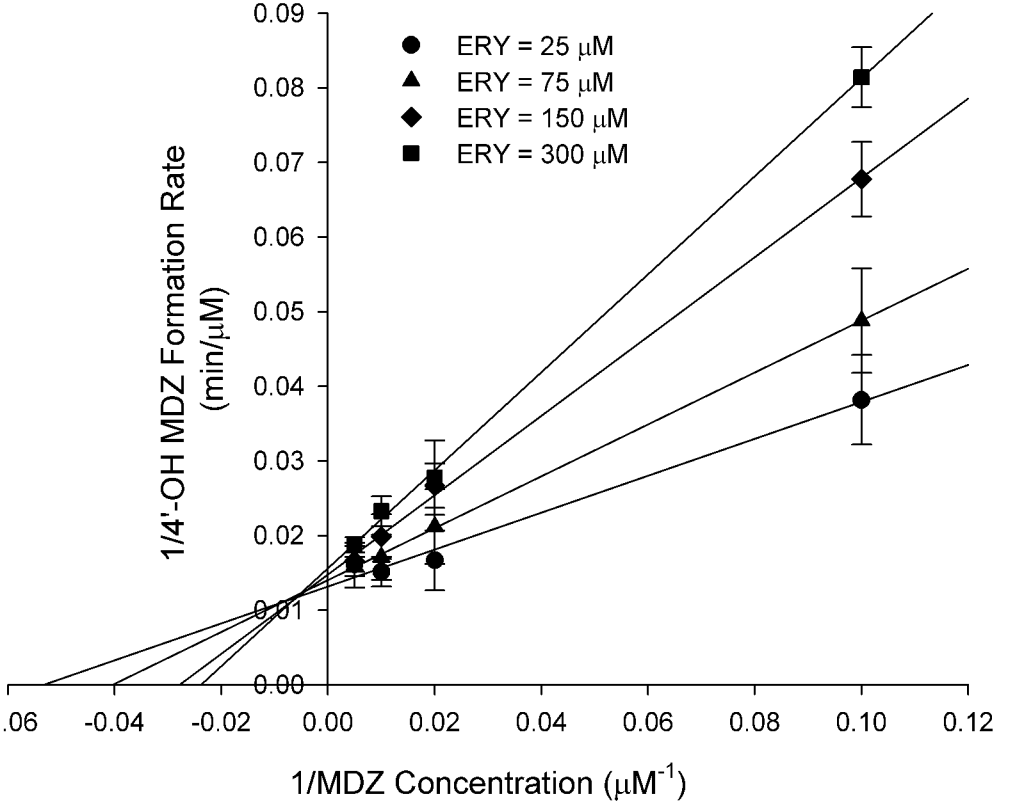
ERY = 25 μM
ERY = 75 μM
ERY = 150 μM
ERY = 300 μM
1/4'-OH MDZ Formation Rate (min/μM)
0.09
0.08
0.07
0.06
0.05
0.04
0.03
0.02
0.01
0.00
-0.06
-0.04
-0.02
0.00
0.02
0.04
0.06
0.08
0.10
0.12
1/MDZ Concentration (μM-1)

DMD Fast Forward. Published on October 1, 2009 as DOI: 10.1124/dmd.109.028290
This article has not been copyedited and formatted. The final version may differ from this version.

Figure 6

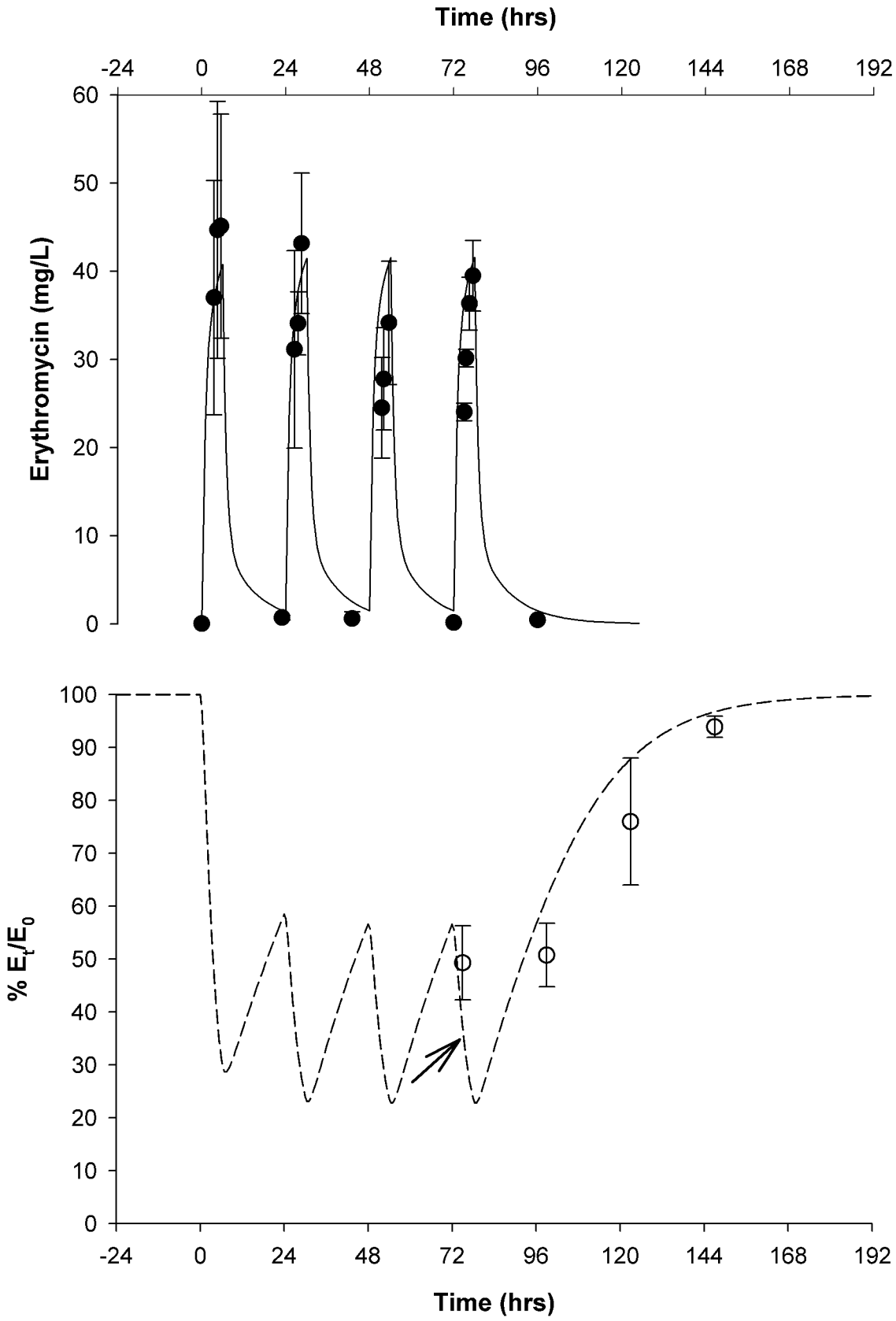

Fig. 7

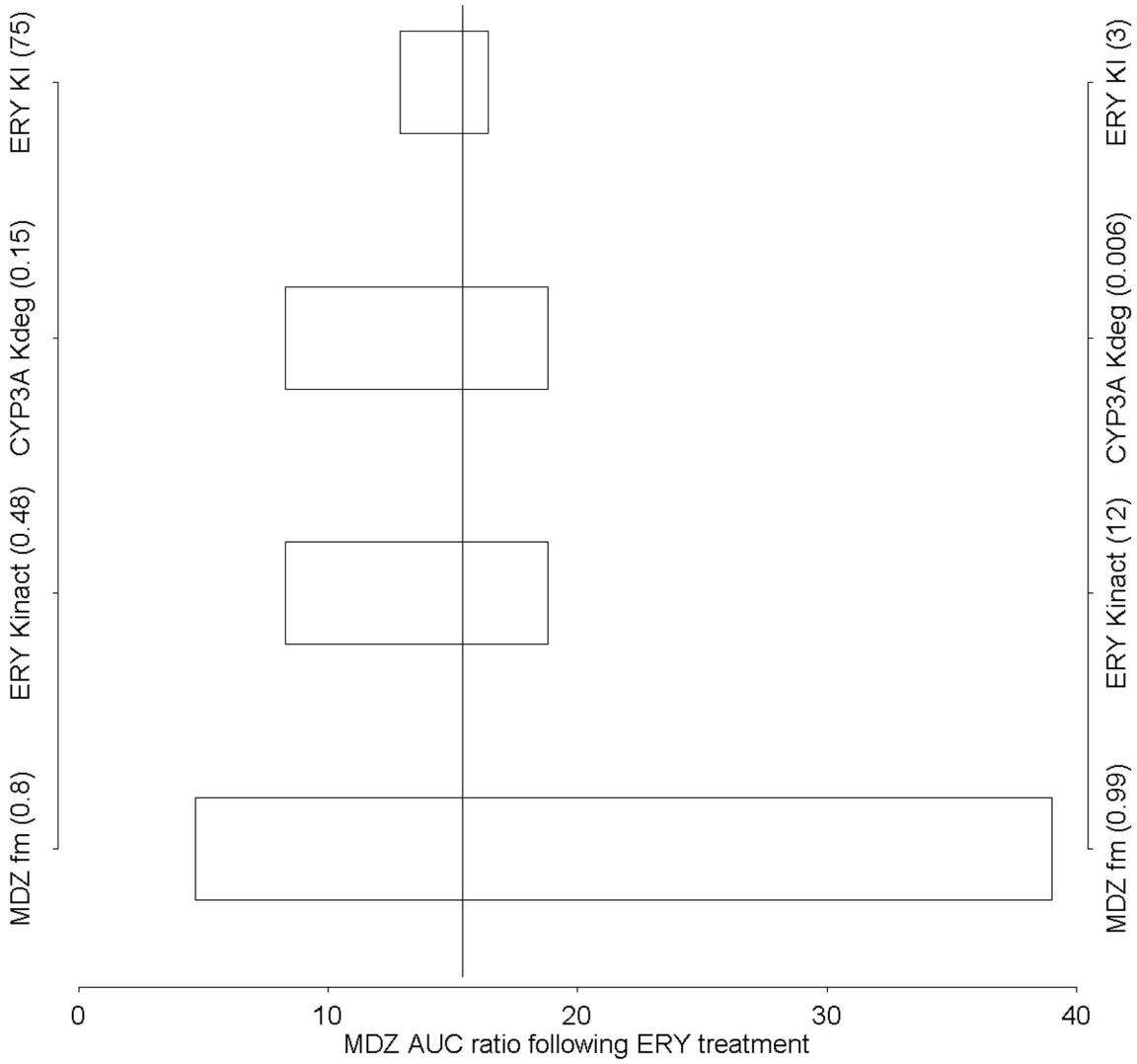
ERY KI (75)
CYP3A Kdeg (0.15)
ERY Kinact (0.48)
MDZ fm (0.8)
ERY KI (3)
CYP3A Kdeg (0.006)
ERY Kinact (12)
MDZ fm (0.99)
0
10
20
30
40
MDZ AUC ratio following ERY treatment

DMD Fast Forward. Published on October 1, 2009 as DOI: 10.1124/dmd.109.028290
This article has not been copyedited and formatted. The final version may differ from this version.

Appendix

Equations used for the estimation of the pharmacokinetic parameters of MDZ

$$V_C = \frac{Dose}{A + B} \quad \text{Eq. A1}$$

$$V_{SS} = V_C \times \left(1 + \frac{k_{12}}{k_{21}}\right) \quad \text{Eq. A2}$$

$$V_{PER} = V_{SS} - V_C \quad \text{Eq. A3}$$

$$k_{21} = \frac{A \times \beta + B \times \alpha}{A + B} \quad \text{Eq. A4}$$

$$k_{12} = \alpha + \beta - k_{21} - k_{el} \quad \text{Eq. A5}$$

$$k_{el} = \frac{\alpha \times \beta}{k_{12}} \quad \text{Eq. A6}$$

where V_{ss} is the volume of distribution at steady state and k_{el} is the elimination rate constant from central compartment.